Designing nickel- and palladium-based precatalysts to improve catalyst-transfer polymerization towards conjugated polymer synthesis

Jeffrey Buenaflor

A dissertation

submitted in partial fulfillment of the

requirements for the degree of

Doctor of Philosophy

University of Washington

2019

Reading Committee:

Christine K. Luscombe, Chair

Brandi M. Cossairt

Gojko Lalic

Program Authorized to Offer Degree:

Chemistry

University of Washington

Abstract

Designing nickel- and palladium-based precatalysts to improve catalyst-transfer polymerization towards conjugated polymer synthesis

Jeffrey Paz Buenaflor

Chair of the Supervisory Committee:
Professor Christine K. Luscombe
Material Science & Engineering

Catalyst transfer polymerization (CTP) is a versatile synthetic tool to obtain access to sequence specific π-conjugated polymers, which are attractive materials for organic electronics. CTP proceeds through a chain-growth mechanism creating polymers with precise molecular weights, narrow dispersities, and end-group functionalization. These parameters are desirable properties that can affect the overall performance of organic electronic and photonic devices. While CTP has made large advances in the synthesis of π-conjugated polymers in the past 15 years, its substrate scope has been limited to mainly simple and electron rich monomers. The need to expand the scope of CTP to access more complicated conjugated building blocks, such as alternating donor-acceptor monomers, necessitates the need to develop new strategies. This report presents an approach to improve CTP by exploring a model study involving nickel and palladium precatalysts to test the

impact of cooperative catalysis and non-covalent π-π stacking interactions on the important metal π-aryl complex. Catalyst performance in CTP was evaluated using poly(3-hexylthiophene) as the model system. Monomer conversion, degree of polymerization, end-group identity, and molecular weight distribution were analyzed to determine the quality of the polymerizations. The information gained from this study provided insight into what structural features are desirable when designing a suitable catalyst that will exhibit a controlled polymerization.

TABLE OF CONTENTS

LIST OF FIGURES

LIST OF TABLES

ACKNOWLEDGEMENTS

I would like to acknowledge several people during my tenure as a graduate student at UW. To the Luscombe Research Lab, thank you for all the support and great times these past few years. I would particularly like to thank my PI, Professor Christine Luscombe for her guidance, patience, and support. I also would like to thank Hang Qian, and Aum Upadhyay, who were two students I had the opportunity to mentor and teach the art of organic chemistry. I would like to give a shout out to Parker Sommerville and Hang, as they helped contribute to my first author paper, something I never thought I would ever accomplish. Everyone in the research group I worked with these past four years, thank you for the advice and discussions I had in tackling my research projects.

The UW SACNAS Chapter and Women in Chemical Sciences, now known as Inclusion in Chemical Sciences (InCS), have played an important role in helping me get through hard times while in graduate school. My fellow Sacnistas, you have been a huge support for me, cheering me on from the sidelines as I endured some really rough patches. You reminded me so much of my community at CSULA and it made me feel at ease. I will miss this group of phenomenal people. To my colleagues in InCS, both past and present, you have played a very similar role to my SACNAS family, supporting me through my journey while simultaneously trying to finish our rigorous PhD program. I did not connect with many people in our department, but I was able to build some rapport with a few individuals in InCS. I will be forever grateful to several members from both organizations.

There are many colleagues, staff, and faculty I would like to acknowledge as many have guided me through in areas outside of research. These people include Dr. Jasmine Bryant, Professor Pradip Rathod, Dr. Anthony Salazar, Dr. Carolyn Jackson, Dr. Paul Miller, Dr. Debbie Wiegand, Krista Holden, Diana Knight, and Kim Quigley, who are all amazing people. I would like to especially acknowledge Professors Brandi Cossairt and Gojko Lalic who have played a huge role in my early years as a graduate student. They were among many people who helped me during a dark time after I chose to leave my first research group. Thank you for agreeing to be on my committee.

Last, but not least, there are two lovely and brilliant ladies who I want to recognize, Dr. Chloe Lombard and Sujata Chakraborty. These two have been with me through thick and thin and have been my pillars of support. They have been a guiding light these past five years. I really take joy in the fact that we all adopted cats in the same year. I am sad that we are parting ways, but I am glad to have built a strong friendship with you two.

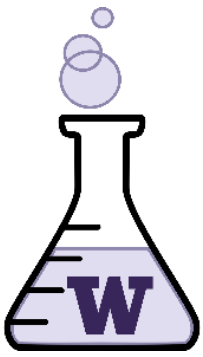

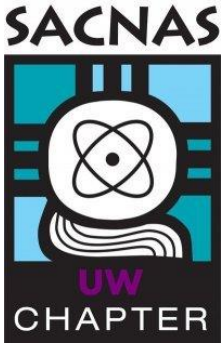

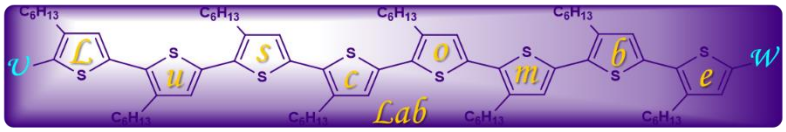

Diversity in
Clean Energy

DEDICATION

I dedicate this dissertation to my “academic mom”, Professor Linda Tunstad

Chapter 1. INTRODUCTION TO CATALYST-TRANSFER POLYMERIZATION AND THE SYNTHESIS OF CONJUGATED POLYMERS

*The work in this chapter has been adapted from a previously published chapter review: "Living polymerizations of π-conjugated semiconductors", Handbook of Conducting Polymers, Fourth Edition, **2019**, DOI:[10.1201/b22235-6] and content published as an article: *Macromol. Chem. Phys.* **2019**, 1900363; doi: 10.1002/macp.201900363

1.1 INTRODUCTION

Since the seminal findings of Yokozawa[1] and McCullough[2], catalyst-transfer polymerization (CTP) has made several advances in the controlled synthesis of π-conjugated polymers, which are attractive targets for organic electronics.[3] The ability to access semiconducting polymers with precise molecular weights, low dispersities, high regioregularity and end-group functionalization is important for tuning the performance of optoelectronic devices.[4–6] Control over these parameters is achievable through CTP since it proceeds in a chain-growth manner. In this method, one monomer at a time is added to the growing polymer chain. The presence of a hypothesized metal-polymer π-complex influences chain-growth behavior by allowing the catalyst to stay adhered to the growing polymer chain.[7–10] CTP is more advantageous over step-growth mechanisms, which do not share the same control over polymerization. For step-growth polymerizations, the resulting dimers, trimers, tetramers, and oligomers that form can subsequently react with each other or with another monomer. This randomness results in the lack of control in polymerization, generates broader molecular weights, and leads to batch-to-batch variability. **Figure 1.1** depicts the difference between chain-growth and step-growth polymerizations.

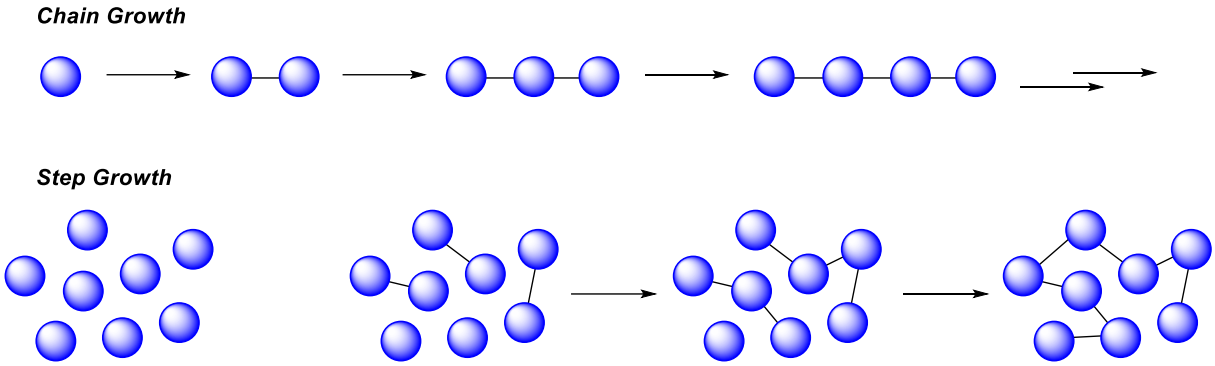

Figure 1.1. Chain-growth *vs* step-growth polymerizations.

The general mechanism for CTP is described in **Figure 1.2** and incorporates steps seen in transition metal catalyzed carbon-carbon cross couplings. CTP encompasses the elementary steps of oxidative addition (OA), transmetallation (TM) and reductive elimination (RE). The hypothesized metal-polymer π-complex is generated after RE. Next, CTP proceeds *via* the catalyst "ring-walking" across the polymer in either direction on the chain until it reaches the next aryl halide bond to initiate intramolecular oxidative addition. The polymer chain is extended through RE after an unreacted monomer is transmetalated onto the polymer metal complex. The polymer continues to grow until the reaction is quenched by an external source.

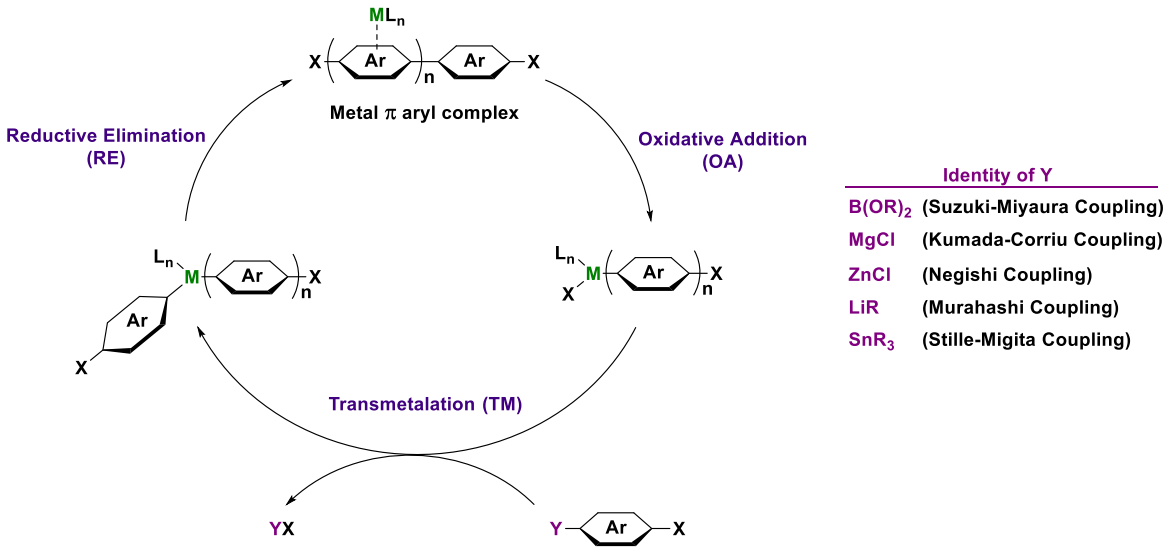

Figure 1.2. General mechanism for CTP.

1.2 SYNTHESIS OF CONJUGATED POLYMERS USING CTP

The discovery of CTP has resulted in a variety of conjugated polymers with different architectures and topologies that consist of block, alternating, or branched copolymers (**Figure 1.3**).[11] While CTP has advanced the field of π-conjugated polymer synthesis, however, its scope has been limited to simple and electron-rich monomers.[9] Progress has been made to use electron-deficient monomers, but successful CTP methodologies remain scarce.[12–15] Success or failure of CTP is strongly dependent on the stability of the metal-polymer π-complex. A weaker metal-polymer π-complex has been observed with electron deficient monomers in CTP. This weaker interaction can result in increased chain termination, thus necessitating the need to develop new strategies for CTP. Overcoming this issue in CTP is especially for important for accessing more complexed systems, such as alternating donor-acceptor (D-A) copolymers, which are of attractive interest in organic electronics due to their favorable properties of high charge mobilities, lower band gaps, and solution-processability.[16–18]

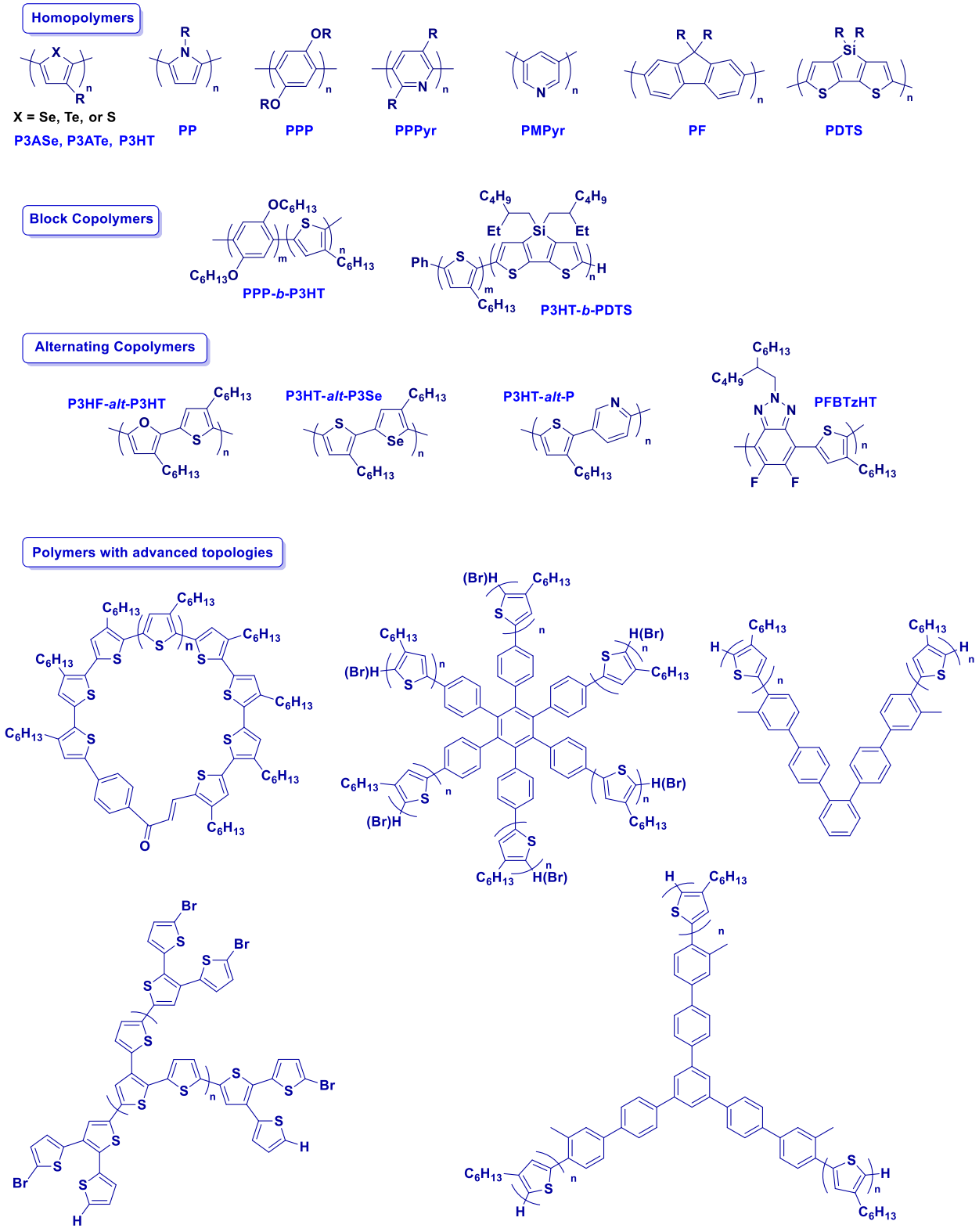

Figure 1.3. Polymers synthesized through CTP.

1.3 IMPROVING CTP

To further advance the field of conjugated polymers using CTP, a better understanding of monomer-catalyst interactions is essential.[19] Recent studies to improve the methodology of CTP primarily focused on the reactive ligands, ancillary ligands, and the transition metal (**Figure 1.4**).[10,19–26] The ancillary ligand has steric and electronic influence over the stability of the π-aryl complex. The reactive ligand provides end functionality, initiates CTP, and provides solubility. Tuning the steric bulk or electronic character of the reagents used in CTP can lead to different results in the synthesis of conjugated polymers. Both sterics and electronics can influence the catalytic cycle by either slowing or speeding up TM, OA, and RE. Additionally the stability of the metal-polymer π-complex can be affected by sterics and electronics.

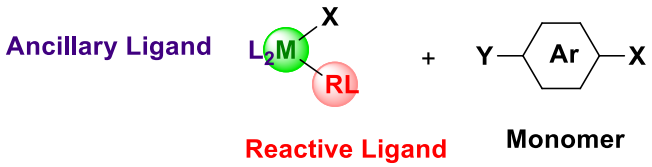

Figure 1.4. The relevant substrates of CTP.

1.3.1 *Modulation of electronic and steric effects in CTP*

McNeil et al. investigated the ligand effects on the Ni catalyst by altering the electronics or sterics of the phosphine groups. They found that the rate-determining step in Kumada catalyst-transfer polymerization (KCTP) can change depending on the catalyst employed in the polymerization. **Figure 1.5** displays the Ni catalysts used in the electronic and steric studies.[19–21,27] **Table 1.1** shows the rate-determining step for KCTP for each of the employed catalysts. Ni(dppp)Cl_2 and Ni(dppe)Cl_2, which are commonly used initiators for KCTP, influence the mechanism differently. The rate-determining steps with the two catalysts are transmetalation and reductive elimination, respectively. Sterics are attributed to be the major influence these ligands

have on the mechanism of KCTP. The main structural differences between the two bidentate ligands are bite angle (dppp = 91°; dppe = 85°) and chelate ring size (six vs. five). Bite angles and cone angles are influenced by the steric bulk of ligands. Different observations seen through the addition of LiCl confirmed the effect of having different rate-determining steps in KCTP. When transmetalation is the rate-determining step, the monomer is directly involved. The addition of LiCl increases the propagation of polymerization through the formation of Grignard ate complexes.[28,29] The addition of LiCl to KCTP initiated by Ni(dppe)Cl_2 has no effect on the polymerization rate, since the monomer is not involved in reductive elimination.

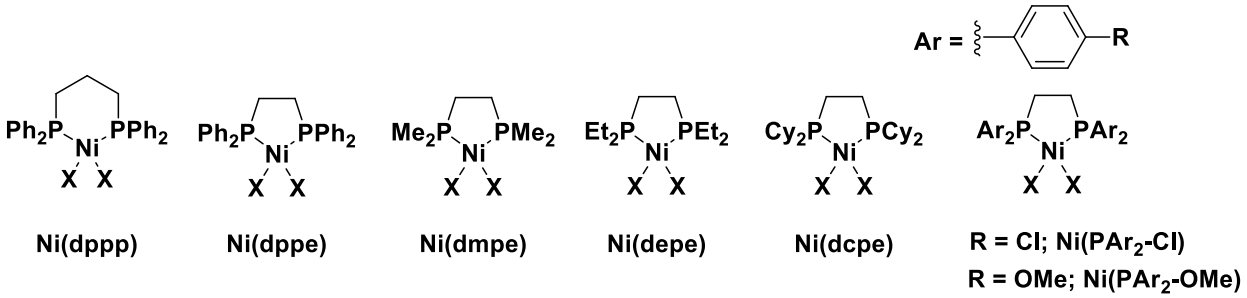

Figure 1.5. List of Ni catalysts with varying phosphine ligands.

Table 1.1. Effect on KCTP mechanism through choice of catalyst ancillary ligand.

Catalyst	Rate-determining step in KCTP
Ni(dppp)	Transmetalation
Ni(dppe)	Reductive elimination
Ni(depe)	Transmetalation
Ni(dmpe)	Reductive elimination
Ni(dcpe)	Transmetalation
Ni(PAr_2-Cl)	Reductive elimination
Ni(PAr_2-OMe)	Reductive elimination

Further studies on catalysts with bis(diakylphosphino) ethane-based ligands [dmpe = 1,2-bis(dimethylphosphino)ethane, depe = 1,2-bis(diethylphosphino)ethane, and dcpe = 1,2-bis(dicyclohexylphosphino)ethane] of varying steric bulk were investigated. Polymerization with Ni(dmpe)Cl_2 is ineffective due to catalyst decomposition. Oligomers were primarily formed with the more sterically bulky Ni(dcpe)Cl_2. This observation was due to the dissociation of the Ni(0) π-aryl complex, allowing for side reactions to occur. The rate-determining step for Ni(dcpe)Cl_2 is transmetalation, which was expected since steric bulk increases the rate of reductive elimination to relieve the strain while slowing transmetalation. Ni(depe)Cl_2 synthesized P3HT and poly-(*para*-phenylene) (PPP) through chain-growth similar to Ni(dppe)Cl_2, albeit with different polymerization rates. These two catalysts have similar bite and cone angles, suggesting the influence of ligand-based electronics, since the depe ligand is more electron donating than dppe.

The influence on ligand electronics was followed up with the usage of electron donating and withdrawing groups on the aryl substituents of the phosphine ligands (**Figure 1.6**).[20] **Table 1.2** displays the polymerization results with the different Ni catalyst. Using an electron donating moiety had the most beneficial effect on polymerization performance. A narrower molecular weight distribution was achieved compared to standard dppe and Ar-Cl catalysts. The increased electron density from the Ar-OMe modified Ni catalyst increased the rate of oxidative addition and the stability of the associative Ni(0) π-aryl complex, thus minimizing termination and interchain transfer reactions.

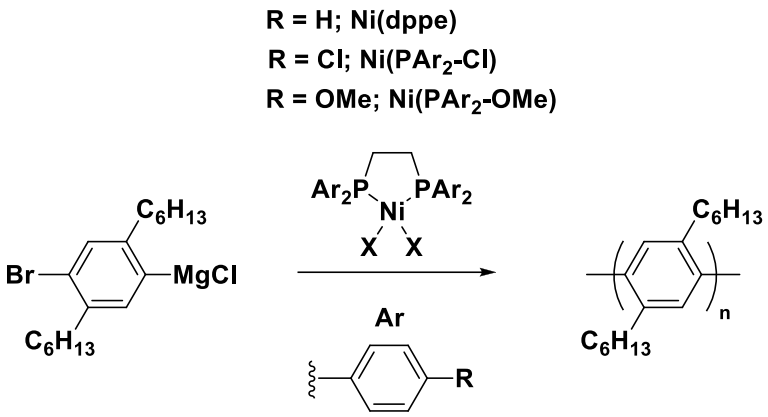

Figure 1.6 Synthesis of poly-*para* phenylene (PPP) using varying Ni catalysts.

Table 1.2. Polymerization results comparing Ni catalysts with different electronic properties.

Catalyst	M_n (kg/mol)	*Đ*
Ni(dppe)	20.1	1.46
Ni(PAr_2-Cl)	19	1.74
Ni(PAr_2-OMe)	16	1.29

1.3.2 *Modifying the stability of the metal-polymer π-complex in CTP*

The electronic character of the monomer also influences CTP, specifically the stability of the metal π-aryl complex. When the complex is very stable or unstable, intramolecular transfer for oxidative addition is hindered. This is due to either the dissociation or trapping of the Ni(0) catalyst. Controlled polymerizations in CTP have typically employed electron-rich monomers, such as thiophenes. On the other hand, examples of controlled polymerizations with n-type monomers *via* CTP are limited. It has been reasoned that the weaker π-donation from the n-type polymer backbone hinders intramolecular transfer for oxidative addition due to a less stable metal π-aryl complex.[12,13,30] Alternatively, it has been suggested that preferential binding of the catalyst on electron-deficient arenes inhibits oxidative addition.[31–33] This hypothesis can be attributed to π-backbonding, which is known to be stronger with electron-poor ligands as observed with alkenes.[34]

Computational studies by Bilbrey showed an elongation of the unsaturated C-C bond on the thiophene, indicating the occurrence of π-backbonding with the metal π-aryl complex.[35] For either scenario, chain termination reactions start to become competitive, reducing control over polymerization. For the synthesis of poly(pyridine-2,5-diyl), Yokozawa et al. observed the dissociation of the Ni catalyst. It was proposed that coordinations between the pyridine nitrogen and the Ni metal center of two monomers resulted in an increased tendency for disproportionation.[30] Another example of catalyst dissociation involving the synthesis of a P3HT-pyridine copolymer will be discussed in a later section. Examples of a very stable metal-polymer π-complex were observed in the attempted polymerization of thiophene-benzothiadiazole-thiophene, thienothiophenes and *p*-phenylene vinylenes (**Figure 1.7**).[31,34,36] The very stable metal-polymer π-complex prevented polymerization from occurring as the Ni catalyst remained trapped and unable to perform the subsequent oxidative addition. Pd metal containing catalysts were able to polymerize the thienothiophenes monomer, due to the weaker association of Pd(0) intermediate to the polymer backbone.[34] It is worth noting that thienothiophenes are electron-rich monomers, while benzothiadiazole is electron-deficient. It is not clear as to what is the dominating factor that leads to a stable metal π-aryl complex, and that it may vary depending on the monomer and ligand structure.

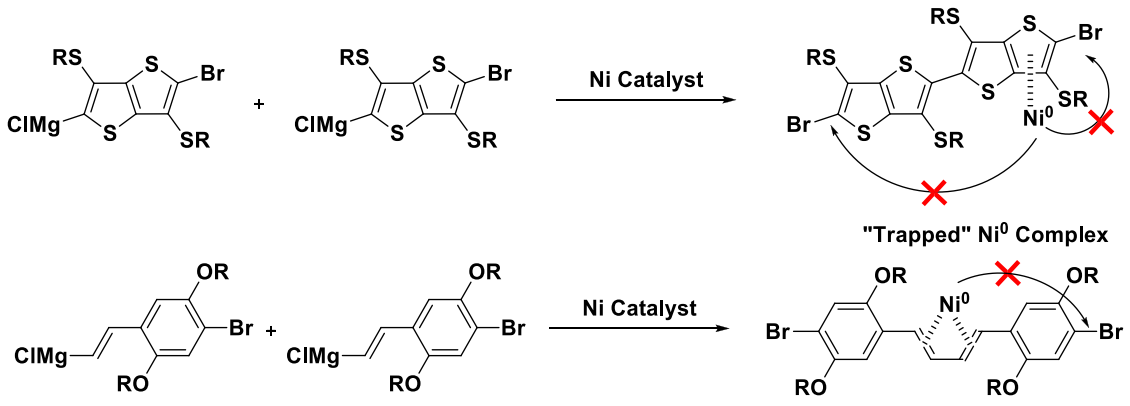

Figure 1.7. Trapping of Ni(0) aryl complex

Further investigations in this area of CTP by Seferos et al. provide more insight on the importance of the stability of the metal π-aryl complex.[15] Using diimine Ni catalysts for their similar election-donating properties to phosphines and ease of modification at the 2-position, Seferos et al. developed a series of catalysts that varied in electronic character and ran polymerizations on a benzothiadiazole monomer.[15] Additionally, computational studies were used to measure the relative stability of the associative Ni(0) π-aryl complexes. The more electron-rich diimine Ni catalyst showed greater degree of control over dispersity and molecular weight.

1.4 OUTLOOK OF CTP AND BEYOND

Much progress has been made in improving CTP, however, the field remains limited in monomer scope. Despite the advances gained in mechanistic insight of CTP, monomer-catalyst interactions are a critical factor that has impeded the design of efficient catalysts. While broadening the substrate scope in CTP beyond simple monomer scaffolds is desirable in expanding the synthesis of conjugated polymers, many challenges are immediately faced by switching the electron rich monomer with electron deficient substrates. The disparity between the growth in structural diversification of monomers and compatible catalyst for a controlled polymerization heightens the need to develop new methods. Matchmaking the ideal combination of catalyst and monomer is crucial in achieving a controlled polymerization of π-conjugated semiconducting polymers.

1.4.1 *Exploring CTP using multimetallic cooperative catalysis and non-covalent electrostatic interactions from ancillary ligands*

Interestingly, one area that has not been relatively explored at all in CTP and may be useful is multimetallic cooperative catalysis. Multimetallic cooperative catalysts have been employed to improve the quality of olefin[37–39] and epoxide[40] polymers (**Figure 1.8**). In these studies, the geometry of the bimetallic catalysts and the proximity of the metal centers were suggested to have critical influence on catalytic rates, branching, chain transfer, and control over molecular weight and dispersity. Rigid bridging scaffolds and bulky substituents forced the metal centers to adopt conformations that place their coordination spheres close together. This preorganization is reminiscent of the conformational control observed in enzymes. There is much to be gained from analyzing the ingenuity behind the design of these bimetallic catalysts. To our knowledge, multimetallic cooperative catalysis has not been used in CTP of π-conjugated polymers.

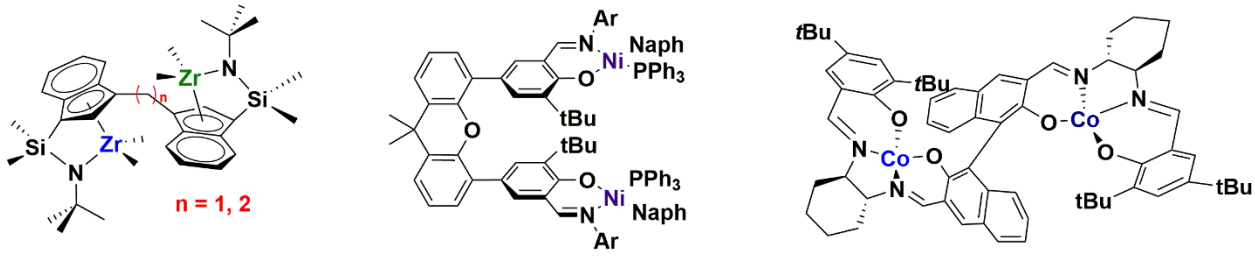

Figure 1.8. Structures of bimetallic catalysts used for olefin and epoxide polymerizations.[37–40]

The use of additional non-covalent electrostatic interactions as a potential to improve CTP is focused on the stabilization of the metal π-aryl complex. As mentioned previously the π-interaction between the polymer and catalyst is influenced by sterics and electronics. π-Stacking interactions have been investigated in N-heterocyclic carbene- (NHC) based metal catalysts.[41] Decorating the metal catalyst with π-conjugated ancillary ligands may offer a favorable interaction that can potentially be used in CTP.

This report presents an approach to improve CTP by exploring the impact of cooperative catalysis and non-covalent electrostatic interactions from the ancillary ligand. To achieve this, two investigations involving a small molecule study with a bithiophene monomer and the synthesis of P3HT *via* KCTP were completed **(Figure 1.9)**. These studies involved several Ni and Pd-based precatalysts (**Figure 1.10**) of varying geometries that were designed to suit each investigation. P3HT was chosen because it is one of the most ubiquitous π-conjugated materials used in organic electronics, and it is extensively known for its high batch-to-batch reproducibility and ease of synthesis.[4] For these reasons, P3HT is a good model system to monitor the success of CTP. Each study is built around influencing the metal π-aryl complex. To evaluate the performance of each catalyst in CTP, we monitored monomer conversion, chain-growth behavior, end-group identity, and dispersity.

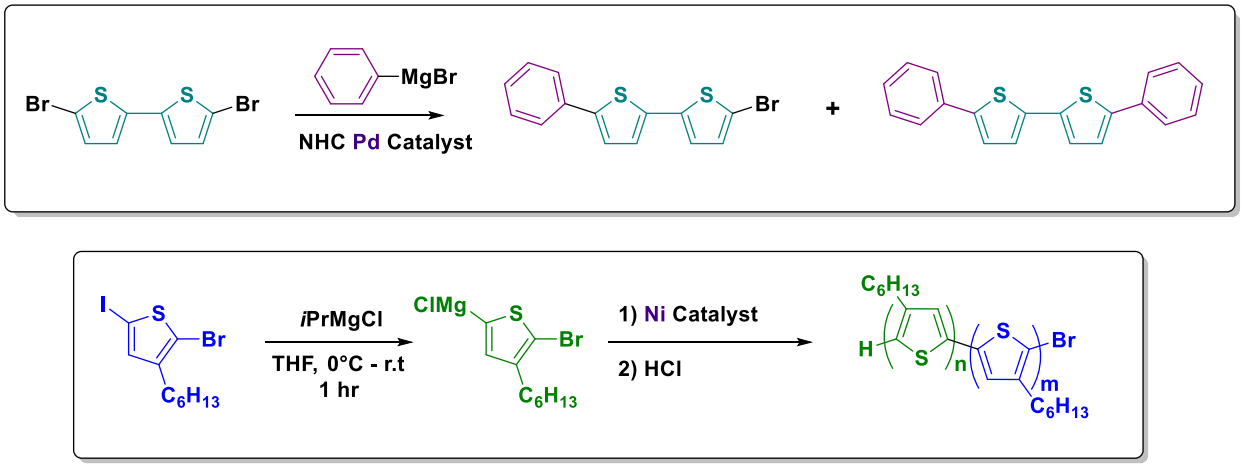

Figure 1.9. The two important reactions used to test the behavior of the Pd- and Ni-precatalysts

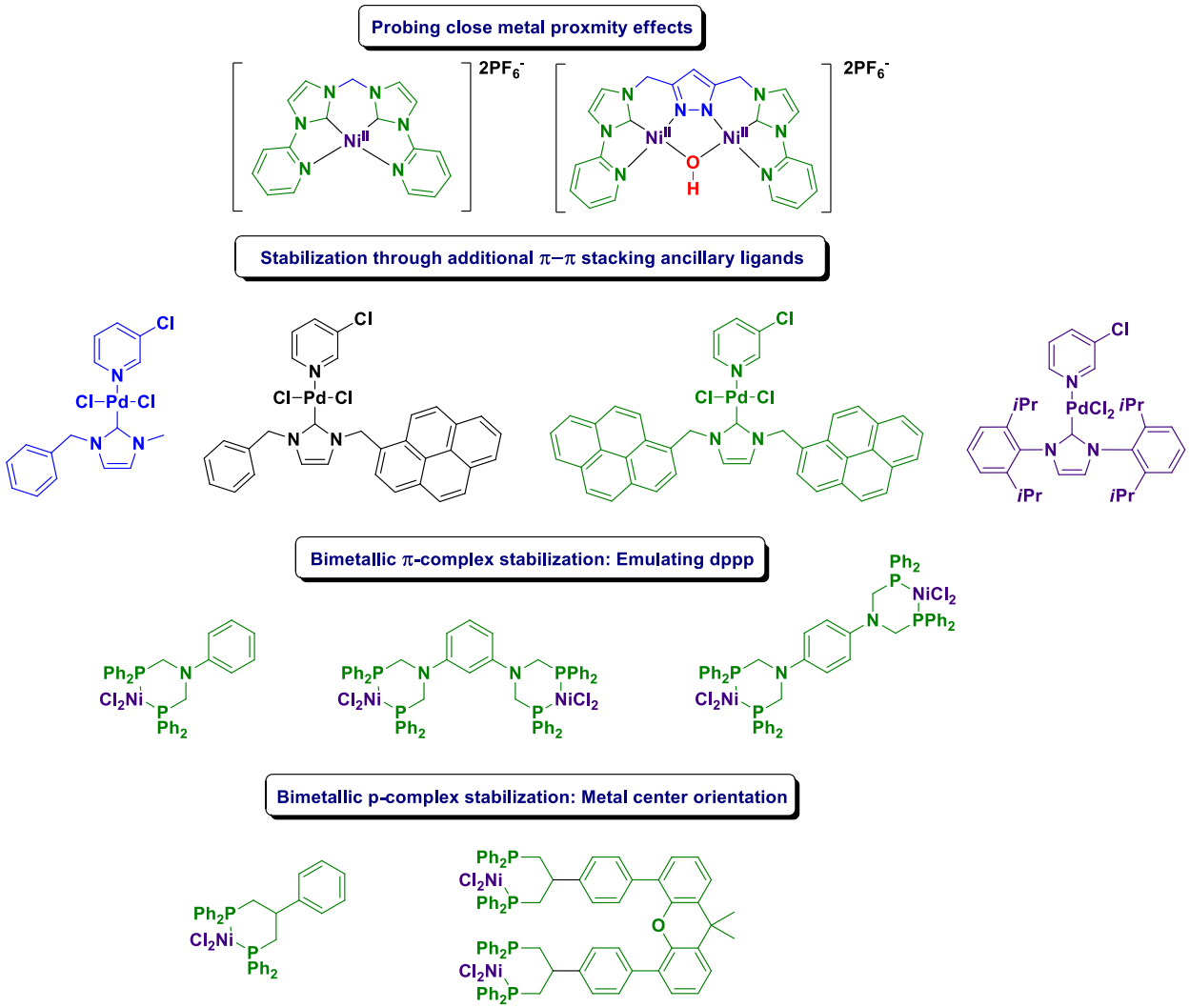

Figure 1.10. Ni and Pd precatalysts investigated in this study.

Maintaining the integrity of the metal π-aryl complex for intramolecular catalyst transfer (**Figure 1.11**) is vital to achieve controlled polymerization in CTP. In KCTP, the metal π-aryl complex is formed after the initiation phase involving two transmetallation steps with an organomagnesio compound, followed by RE. The repeating cycle of OA, TM, and RE as mentioned previously with the general mechanism of CTP occurs until the reaction is quenched with acid. For the synthesis of P3HT through KCTP, the ideal polymer will have H/Br end groups. Polymers that have Br/Br end groups are a result of chain termination processes. Destabilization of the metal π-aryl complex can result in dissociation of the catalyst, which leads to Br/Br end

groups on P3HT. Another interchain termination is disproportionation where two polymer chains are combined through transmetallation resulting in Br/Br polymers and release of the catalyst. Free catalyst reduces uniformity as another polymer can be initiated. The mitigation of chain termination is ideal for controlled KCTP. In this study, we monitored the behavior of these catalysts and analyzed extend of chain termination processes to evaluate the success of KCTP. By testing these catalysts designs, we hope to determine parameters that will be optimal for the viable synthesis of π-conjugated polymers through CTP. **Figure 1.12** represents our envisioned goal of exploring multimetallic cooperative catalysis and non-covalent electrostatic π- π interactions to provide a potentially stabilizing effect that may strengthen the metal π-aryl complex.

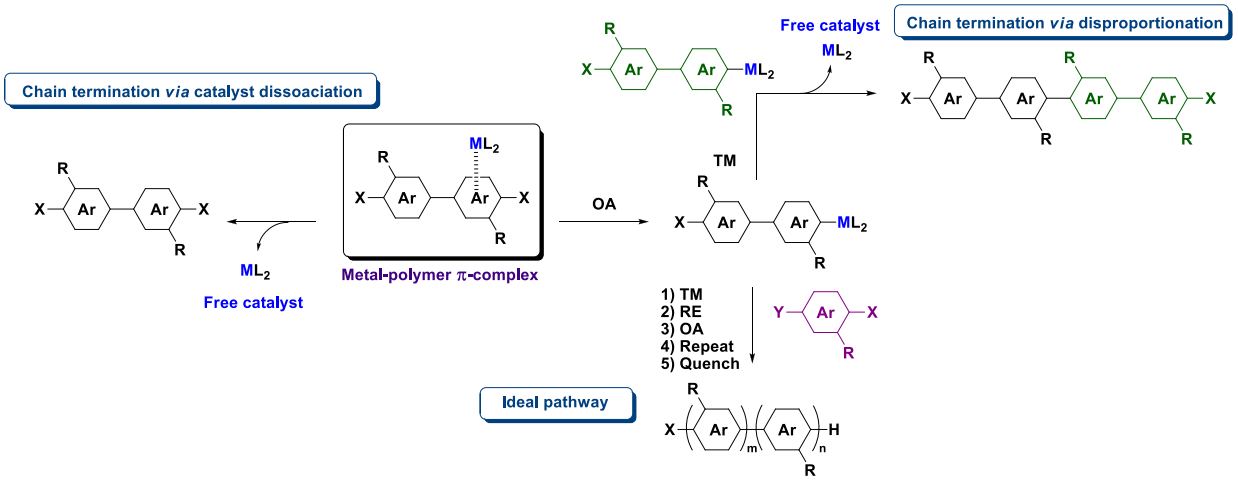

Figure 1.11. CTP mechanism showing the important metal-polymer π-complex.

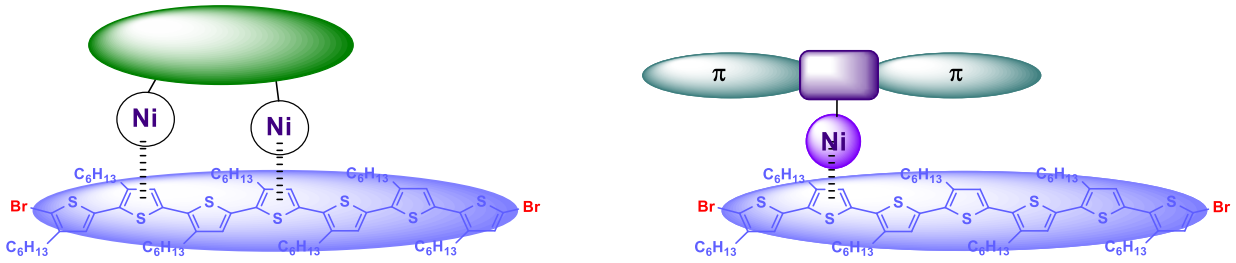

Figure 1.12. Focal points of this study: cooperative metal catalysis and ancillary ligand π-π stacking.

Chapter 2. INITIAL STUDY OF MULTIMETALLIC COOPERATIVE CATALYSIS IN CTP USING *N*-HETEROCYCLIC CARBENE NICKEL PRECATALYSTS

2.1 INTRODUCTION

N-heterocyclic carbene ligands are known for their stability,[42] ease of handling, and in most cases more electron-donating than phosphines.[43] In our preliminary studies to investigate cooperative catalysis, metal proximity, ligand chelation, and stabilization effects were taken into consideration in choosing catalysts to investigate. We conducted a comparative study between monometallic **1** and bimetallic **2** nickel precatalysts (**Figure 2.1**) and utilized them to initiate the synthesis of P3HT. Mononuclear Ni catalyst **1** and bimetallic Ni catalyst **2** have been previously employed in Suzuki and Kumada couplings where they displayed exceptional catalytic activities with aryl halides.[44–46] In this study, we probed the effects of having the two metal centers in close proximity to ascertain their behavior on CTP. The strong σ-donation capabilities to coordinate and stabilize the metal center[47] were promising in influencing the strength of the metal π-aryl complex. The multi-dentate structures of catalysts **1** and **2** are ideal in potentially preventing chain-termination processes.

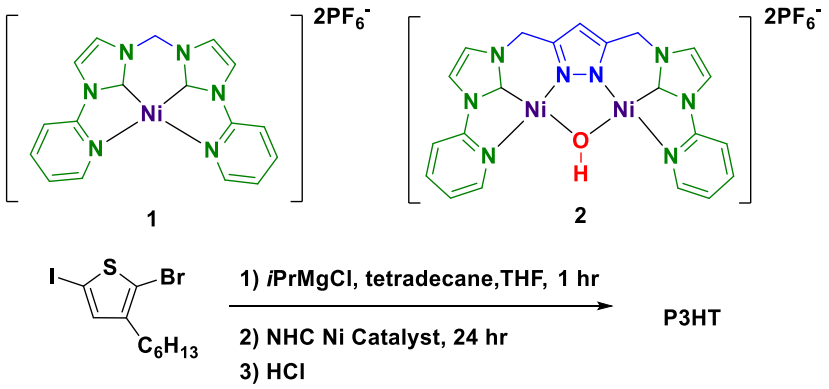

Figure 2.1. Target NHC Ni catalysts **1** and **2**, and synthesis of P3HT.

A comparative study between the two NHC catalysts was conducted to evaluate their performance in CTP. As a frame of reference, the NHC Ni catalysts were compared Ni(dppp)Cl_2. The success of CTP can be monitored by analyzing molecular weight, dispersity, monomer conversion, and end-group distribution on P3HT. These values were determined using characterization tools, such as NMR, SEC, MALDI-TOF, and GC-MS.

2.2 EXPERIMENTAL

2.2.1 *Materials and general spectral information*

Syntheses of the nickel catalysts and their ligand precursors were based on previously reported procedures (**Figures 2.2** and **2.3**).[44,45,48,49] All chemicals used were obtained from commercial suppliers (Sigma-Aldrich, Fisher Scientific, ACROS, VWR, TCI). Solvents were obtained from Pure Solv dry stills or redistilled before use. Reactions were carried out using Schlenk lines under in N_2 when necessary. All synthesized compounds were purified through standard techniques such as flash chromatography, recrystallization, extraction, or filtration. The NMR spectra were obtained from Bruker 300 or 500 MHz AVance series instruments. The mass spectra for compounds with molecular weight above 500 were obtained on a MALDI-TOF Bruker Autoflex II instrument with a 337 nm laser and 2,2':5'2"-terthiophene as the solid matrix. Compounds with molecular weight below 500 and kinetic studies were characterized using an Agilent 5973 GC-MS instrument.

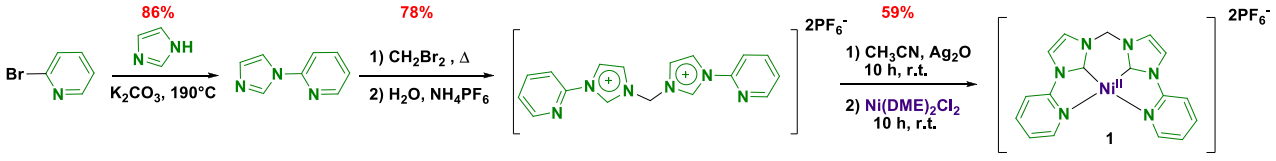

Figure 2.2. Synthesis of Monometallic Ni Catalyst **1** with reported yields.

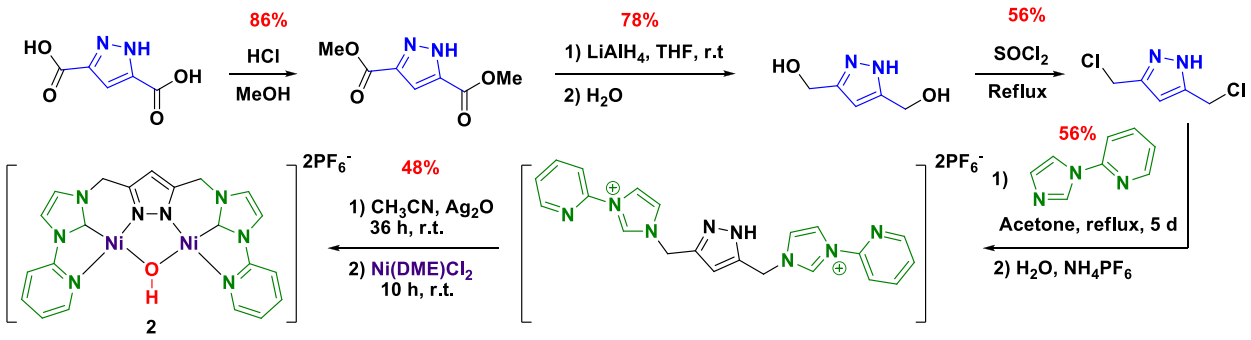

Figure 2.3. Synthesis of Bimetallic Ni Catalyst **2** with reported yields.

2.2.2 *Procedure for synthesis of P3HT and kinetics*

Tetradecane (13 µl, 0.05 mmol), was added to a flask containing 2-bromo-3-hexyl-5-iodothiophene (0.22 mL, 1 mmol). After adding anhydrous THF (10 mL) *via* syringe under N_2, the reaction was cooled to 0 °C. Isopropylmagnesium chloride (2.0M in THF, 0.95 mmol) was added dropwise to the reaction flask. The cooling bath was removed, and the reaction was stirred at room temperature for one hour. NHC catalyst (0.02 mmol) was added directly to the reaction flask to initiate polymerization.

Measured aliquots of 0.3 mL were taken from the reaction at selected times. The time zero point is an aliquot taken from the reaction solution right before the catalyst was added. Each aliquot was quenched using aq. HCl (1.0-3.5 M) and diluted with 1.0 mL of chloroform. 0.1 mL of the chloroform solution was extracted and diluted to 1.5 mL to a GC vial (0.002 M).

2.3 Results and Discussion

2.3.1 *GC-MS kinetic studies*

Polymerization kinetics were completed on both NHC catalysts and Ni(dppp)Cl_2 as a control. The results of the kinetic studies are shown in **Figure 2.4** where the conversion of 2-bromo-5-chloromagnesio-3-hexylthiophene was monitored using GC-MS with tetradecane as the

internal standard. Figure 2.2 displays the progress of the polymerization for three hours with Ni(dppp)Cl_2 and 24 hours with the NHC catalysts. As the reaction progresses, percent monomer remaining decreases. Since NHC catalysts **1** and **2** have never been employed in the synthesis of P3HT, a time span covering 24 hours was selected to give ample time for the reaction to occur. Ni(dppp)Cl_2, which is a common catalyst for KCTP is typically completed in 1.5 hours. Monomer conversion for both monometallic catalyst **1** and bimetallic catalyst **2** was very low in the course of 24 hours. Compared to Ni(dppp)Cl_2, which had 78% monomer conversion by the 2 hours, the low conversions with the NHC catalysts suggests polymerization is halting prematurely due to chain-termination processes.

The slow monomer conversion for catalysts **1** and **2** are most likely due to steric hindrance from the growing polymer and catalyst ligands. The hemilability of the pyridyl ligand allows it to pop on and off the catalyst leaving a vacant coordination site. However, since it is part of the chelation with the carbene moiety, it is constrained. This restricted ligand conformation may be causing an unfavorable steric interaction with the polymer. This steric interaction was not observed in the previous studies of the catalysts, since they were used to couple small molecules, not polymers. After 22 hours, mononuclear catalyst **1** converted more monomer (27%) than the bimetallic catalyst **2** (22%). Based on the polymerization kinetics, there were no apparent cooperative effects exhibited by having two metal centers.

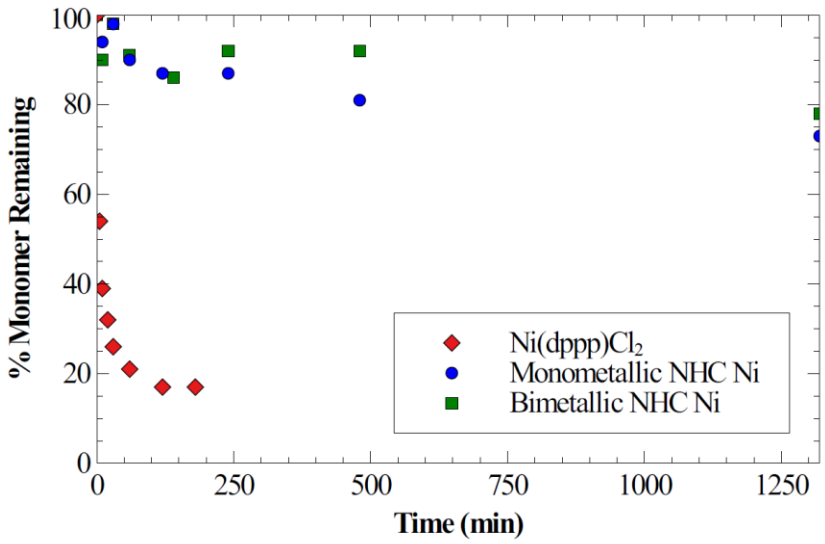

Figure 2.4. Percent monomer remaining *vs.* time plot of 3-hexylthiophene (3HT) polymerization.

2.3.2 *Analysis of CTP behavior*

Table 2.1 displays the degree of polymerization (DP), molecular weight (M_n), and dispersity ($Đ$). The isolated molecular weights of P3HT obtained from the polymerizations initiated by catalysts **1** and **2** match the predicted values calculated from the kinetics. DP was calculated using Equation (1)[50] and **Figure 2.5** displays the ^{1}H-NMR spectra detailing the pertinent peaks needed to complete the calculation. The dispersity of the polymers was analyzed using SEC, and the reported high values indicate uncontrolled polymerization.

Table 2.1. Results of (3-HT) polymerization trials.

Catalyst	Monomer Conversion (%)	Predicted M_n (kg/mol)	Actual M_n (kg/mol)	DP	$Đ$
Ni(dppp)Cl_2	83	6.5	5.2	31	1.26
Monometallic Ni **1**	27	2.3	2.2	13	2.93
Bimetallic Ni **2**	22	1.9	1.7	10	3.43

$$DP = \left(\frac{I_{repeating\ unit}}{\#\ of\ protons\ of\ repeating\ unit} \times \frac{\#\ of\ protons\ of\ end-groups}{I_{end-groups\ and\ regioisomers}}\right) + 2 \qquad (1)$$

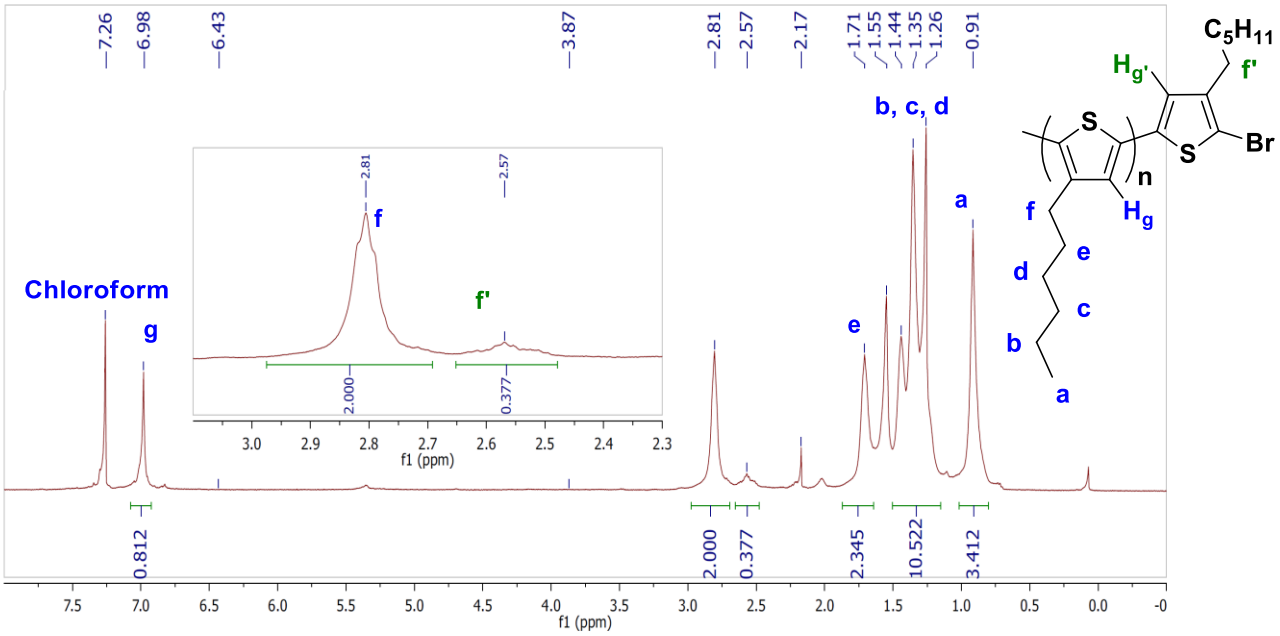

Figure 2.5. Detailed NMR of P3HT synthesized using monometallic Ni catalyst **1**.

End-group analysis was completed using MALDI-TOF. **Figure 2.6** contains the MALDI spectral data for catalysts **1** (a) and **2** (b). Both catalysts display P3HT terminated with H/Br and Br/Br. For both cases, the content of Br/Br end-groups is relatively compared to P3HT synthesized using Ni(dppp)Cl_2 which is known for having a high mitigation of chain termination. Bimetallic Ni NHC catalyst **2** displays a higher ratio of Br/Br P3HT, indicating increased chain termination processes and supporting the notion of an uncontrolled polymerization.

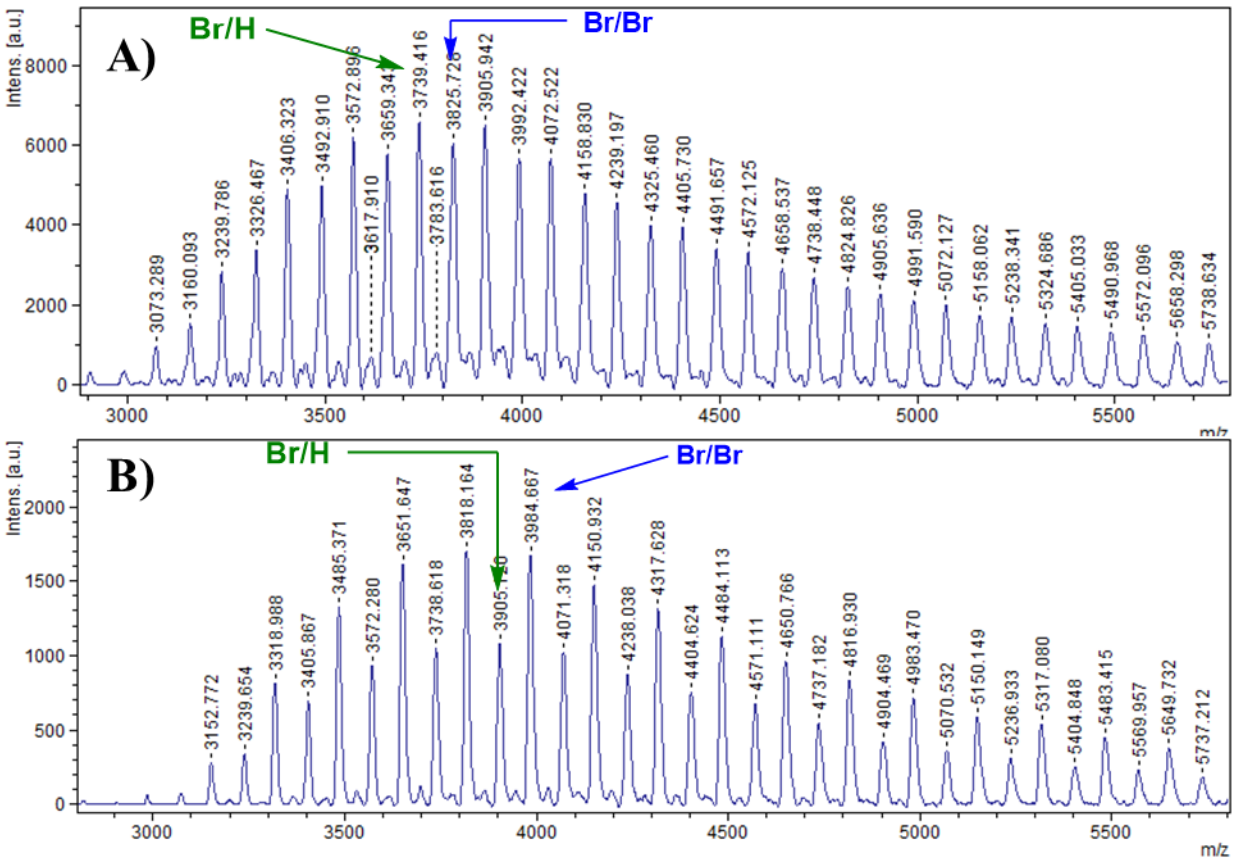

Figure 2.6. MALDI results for monometallic catalyst **1 (A)** and bimetallic Ni Catalyst **2 (B)**.

2.4 CONCLUSIONS

Characterization of the polymerizations initiated with catalysts **1** and **2** resulted in the synthesis of P3HT, however polymer chain length was low compared to Ni(dppp)Cl_2. Analysis of end-group distribution and dispersity of isolated P3HT indicated the polymerizations with the NHC catalysts were uncontrolled. Additionally, bimetallic catalyst **2** did not exhibit any enhanced catalyst activity compared to monometallic catalyst **1**, suggesting there was no cooperativity between the two metal centers. The primary cause for the poor performance of the two NHC catalysts can be tied to sterics, which can slow down transmetallation and destabilize the metal π-aryl complex resulting in increased chain termination processes.

Chapter 3. SMALL MOLECULE STUDY WITH *N*-HETEROCYCLIC CARBENE PALLADIUM PRECATALYSTS CONTAINING Π-CONJUGATED LIGANDS

3.1 INTRODUCTION

Small-molecule model systems have been used to explore CTP to improve existing methods and identify alternative catalysts.[9] Noonan *et al* investigated the utility of a monomer containing an electron-withdrawing ester moiety for Suzuki CTP.[51] They also compared the behavior of PEPPSI-IPr and to $Ni(PPh_3)IPrCl_2$ in their model studies to find suitable catalysts. Another study by Noonan and coworkers focused on Stille CTP small molecule models to scope for evidence for intramolecular oxidative addition, which is the step that occurs in CTP after RE and as the catalyst walks to the next aryl-halide bond.[52] In these model studies, a dihalide system is used as the monomer and is reacted with a stoichiometric amount of a monofunctionalized organometallic monomer. The first coupling represents the initiation phase of CTP where an intermolecular reaction between two aryl substrates are connected after reductive elimination to form the metal π-aryl complex. The second coupling is part of the propagation phase in CTP where intramolecular oxidative addition occurs. This simple strategy provide mechanistic insight for CTP is valuable, however McNeil *et al* advises caution on results obtained through these model studies. In one study, McNeil and coworkers would find that product ratios in the small molecule reactions were determined by reactivity differences in substrates than the associative intermediate π complex.[53] Small molecule model studies in CTP provide information that can infer and inspire future catalyst and substrate designs, but the information might not always translate to successful polymerizations.

The focus of this study is centered on probing the usage of additional π-π electrostatic interactions in CTP. This work was inspired from Suzuki-Miyaura couplings that incorporated pyrene substituents in NHC ligands resulting in enhanced catalytic activity.[54] Ruis-Butella and Peris believed that the π-stacking between the aromatic substrates and the pyrene substituent facilitated an interaction between the substrate and the metal resulting in the enhanced activity. A control study was conducted where free pyrene was added to the reaction resulting in partial inhibition of catalytic activity for complexes that possessed the pyrene ligands. Catalysts that lacked the pyrene substituent were unaffected by the addition of free pyrene. In our study, we wanted to take advantage of the beneficial interaction observed with pyrene substituted ligands and apply it to CTP. We envisioned a favorable interaction that may provide additional stabilization to the metal π-aryl complex (**Figure 3.1**).

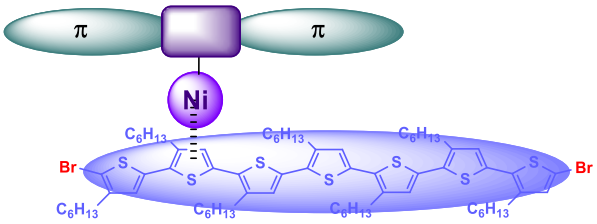

Figure 3.1. Illustration of metal π-aryl complex with π-conjugated ligands.

Our small molecule model study involved a dihalide functionalized bithiophene monomer that was reacted with an organomagnesio compound *via* a Kumada coupling initiated by NHC Pd catalysts. (**Figure 3.2**). We monitored the performance of the NHC catalysts by analyzing the formation of a mono- and di-coupled products. The formation of these products is detailed in **Figure 3.3** and they are designated with the labels "intermolecular" and "intramolecular" as they represent two key components of CTP. The intermolecular product represents the beginning of CTP where the first coupling of the monomer occurs with an intermolecular transfer through OA and RE. The formation of the intramolecular di-coupled product is reminiscent of the

intramolecular OA of the M(0) complex after it walks to the nearest aryl halide bond. By monitoring the formation of these two molecules, we were able to evaluate the performance of each catalyst and determine if they would be suitable for CTP.

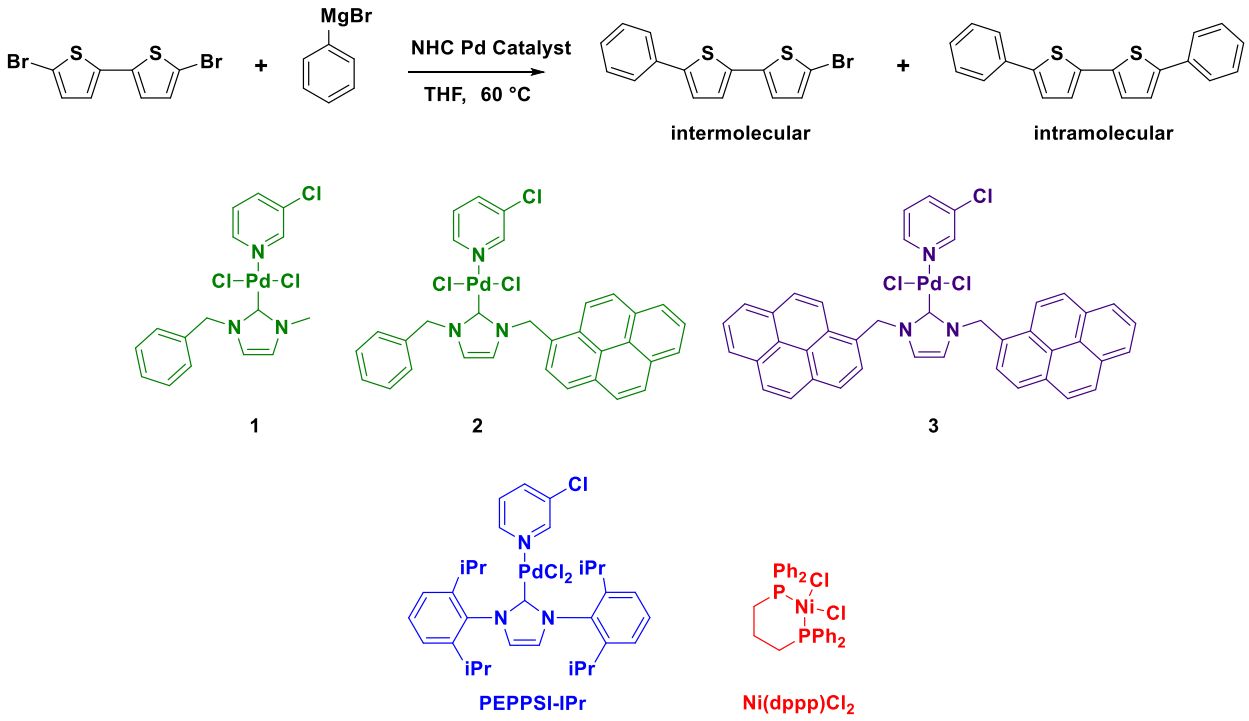

Figure 3.2. Kumada coupling of 2,2'-dibromobithiophene

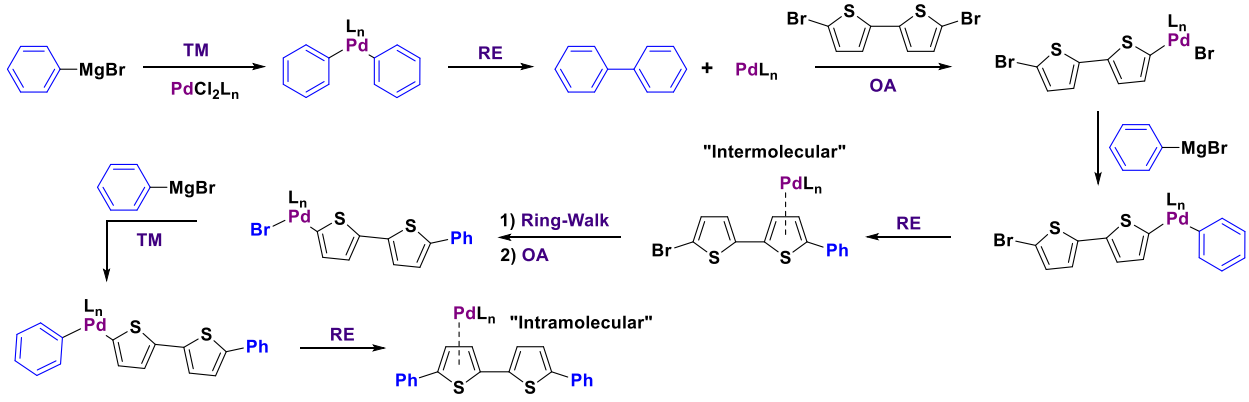

Figure 3.3. Formation of "intermolecular" and "intramolecular" products.

The model study involved three Pd NHC catalysts that vary in the amount of pyrene substituents. The benzyl methyl **1** and benzyl methylene pyrenyl **2** NHC catalysts were previously employed in the Suzuki Couplings. The bismethylene pyrenyl **3** NHC catalyst is our catalyst we designed to test if having the additional pyrene substituent would further enhance catalytic activity and provide further evidence supporting the benefits of the additional π-π stacking. We hypothesized that decorating the catalyst with π-conjugated ligands will generate a favorable interaction that would facilitate intramolecular oxidative addition (**Figure 3.4**). Pd-PEPPSI-IPr was employed as a control experiment for this small molecule model study. Like Ni(dppp)Cl_2, Pd-PEPPSI-IPr is a common catalyst. For NHC ancillary ligands employed in CTP, Pd IPr and SiPr are the only ones used in CTP.[55]

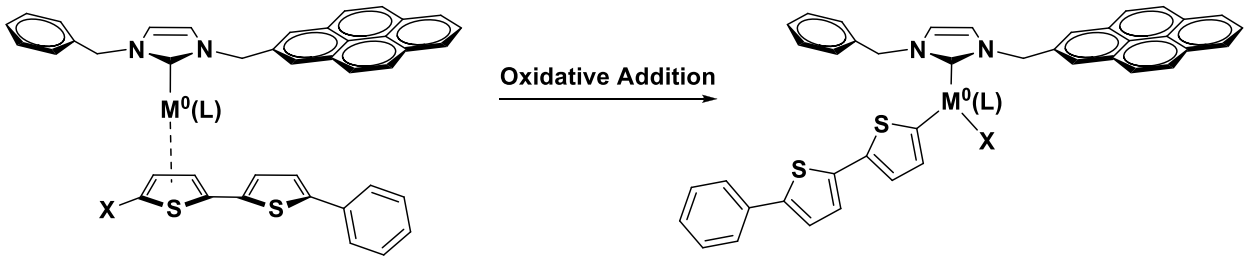

Figure 3.4. Intramolecular oxidative addition into C-X bond.

3.2 EXPERIMENTAL

3.2.1 *Materials and general spectral information*

Syntheses of the Pd NHC catalysts and their ligand precursors were based on previously reported procedures (**Figure 3.5**).[54,56] All chemicals used were obtained from commercial suppliers (Sigma-Aldrich, Fisher Scientific, ACROS, VWR, TCI). Solvents were obtained from Pure Solv dry stills or redistilled before use. Reactions were carried out using Schlenk lines under

in N_2 when necessary. All synthesized compounds were purified through standard techniques such as flash chromatography, recrystallization, extraction, or filtration. The NMR spectra were obtained from Bruker 300 or 500 MHz AVance series instruments. The analysis of the small molecule model study was completed using an Agilent 5973 GC-MS instrument with 1,3,5-trimethoxybenzene as the internal standard.

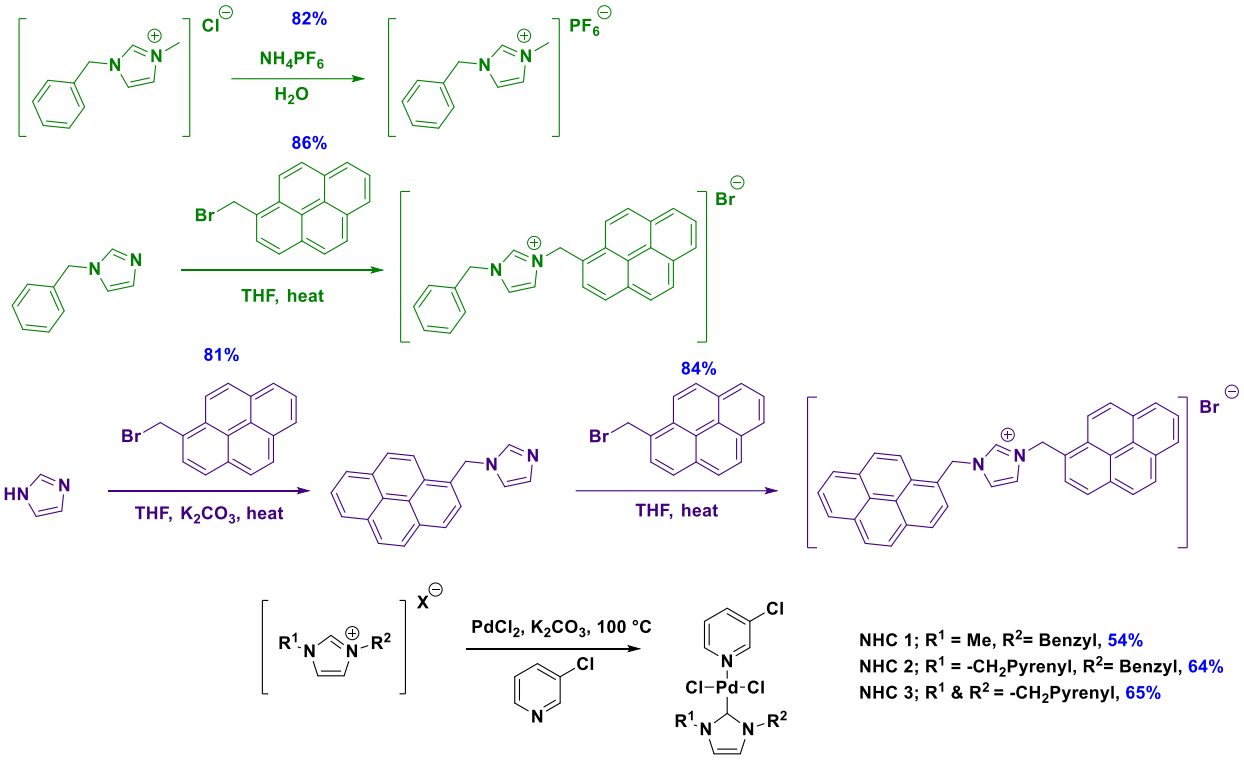

Figure 3.5. Syntheses of imidazolium salts and general reaction to synthesize Pd NHC catalysts.

3.2.2 *Procedure for Kumada coupling of 2,2'-dibromobithiophene*

1,3,5-trimethoxybenzene (2.2 mg, 0.013 mmol), 2,2'-dibromobithiophene (32.4 mg, 0.10 mmol) and catalyst (0.005 mmol) were added into a 4 mL vial. The reaction vessel was purged with N_2 and dry THF (2 mL) was added *via* syringe. An aliquot (0.1 mL) of the reaction mixture was collected for GC-MS analysis. After pre-heating reaction vessel to 60 °C, phenylmagnesium bromide 3.0 M in ether, 0.10 mmol) was added *via* syringe. After 2 hours have elapsed, another

0.1 mL aliquot was removed from the reaction, quenched, and analyzed using GC-MS. The reaction was quenched with 2.0 M HCl.

3.2.3 *Synthesis of P3HT using Pd NHC catalyst **3***

2-bromo-3-hexyl-5-iodothiophene (0.22 mL, 1 mmol) and 1,3,5-trimethoxybenzene (8.4 mg, 0.05 mmol) were added to a reaction flask, which was subsequently placed under high vacuum. After purging with N_2, anhydrous tetrahydrofuran (10 mL) was added *via* syringe. While stirring, the reaction mixture was cooled to 0 °C. Isopropylmagnesium chloride (2.0 M in THF, 0.95 mmol) was slowly added dropwise *via* syringe. After removing the cooling bath, the reaction was warmed to room temperature to stir for an hour. Catalyst **3** (0.042 mmol) was added directly to the reaction mixture. The reaction was stirred at room temperature for approximately 24 hours and quenched with 1.5 mL of 2 M HCl. After 10 minutes have elapsed, the mixture was added to a flask containing excess methanol to precipitate the polymer. The solid was subsequently filtered and washed with methanol and acetone until the filtrate solution was clear. The polymer was collected after drying *in-vacuo*. Th isolated P3HT was characterized by NMR, MALDI and SEC.

The procedure for the kinetic study with catalyst **3** used 1,3,5-trimethoxybenzene (0.05 mmol) was used as a reference standard. Before the catalyst **3** was added, a time 0 aliquot was removed from the reaction mixture. Upon initiating the polymerization, aliquots (0.2 mL) were removed from the reaction over the span of 24 hours and added to a vial containing 1.0 mL of $CHCl_3$. Each aliquot was quenched with aq. HCl (2.0 M). 0.6 mL of the organic layer was extracted into a vial after drying through a filter containing Na_2SO_4. After removing the solvent *in-vacuo*. 0.6 mL of $CDCl_3$ was added to each vial and the solution was analyzed by ^{1}H-NMR. Calculation of predicted M_n is based on Equation (2) and (3) where n = number of repeating units; $[M_i]$ = mmol of Grignard monomer and $[Ni_i]$ = mmol of $Ni(PPh_3)_2Cl_2$ precatalyst.

$$n = \left(\frac{[M_i]}{[Ni_i]}\right) \quad (2)$$

$$M_{n(Predicted)} = n \times (M.W.of\ repeating\ unit) \quad (3)$$

3.3 Results and Discussion

3.3.1 *Small molecule Kumada Coupling: intermolecular vs intramolecular products*

Table 3.1 summarizes the small molecule study with the NHC catalysts. When comparing the catalysts **1 - 3**, bismethylene pyrenyl NHC **3** has the highest intermolecular (Br/Ph): intramolecular (Ph/Ph) products ratio. Interestingly, the intermolecular:intramolecular products ratio of catalysts **1 - 3** are exceedingly low compared to Pd-PEPPSI-IPr and Ni(dppp)Cl_2. This major difference in product ratios was unfortunately unpromising for using the catalysts in CTP. The results indicate catalysts **1 – 3** are poor candidates for CTP. Sterics is most likely the reason for the low performance of catalysts **1 – 3.** In CTP, the ancillary ligand sterics are known for exhibiting a "goldilocks" effect.[9] The ligand cannot be too big or too small or unproductive pathways, such as chain termination processes start becoming more prevalent. PEPPSI-IPr represents the NHC catalyst with the most balanced sterics, thus making it optimal for the CTP. Catalysts **2** and **3** are catalysts with a larger ancillary pyrene ligand, which may be hindering the Kumada Coupling than assisting it with the π-π stacking interaction. Catalyst **1** has a smaller ancillary ligand which can decrease catalyst activity and stability.

Table 3.1. Catalyst performance comparing intermolecular (Br/Ph) and intramolecular (Ph/Ph) product ratios.

Catalyst	Ratio (Br/Ph) : (Ph/Ph)
Bismethylene pyrenyl Pd **3**	1 : 4.43
Bismethylene pyrenyl Pd **3**	1 : 3
Benzyl methylene pyrenyl Pd **2**	1 : 3.60
Benzyl Methyl Pd **1**	1 : 2.63
Pd-PEPPSI-IPr	1 : 16.25
Pd-PEPPSI-IPr	1 : 40.5
Ni(dppp)Cl_2	1 : 30.15

3.3.2 *Polymer kinetics with NHC catalyst **3***

Since NHC catalyst **3** exhibited the highest performance compared to **1** and **2** we employed the catalyst to observe its behavior in KCTP (**Figure 3.6**). **Figure 3.7** summarizes the kinetic study and the results confirm that catalysts investigated for this study are not suitable for CTP. Very little polymer was recovered and analysis of P3HT *via* ^{1}H-NMR revealed a DP of 12.

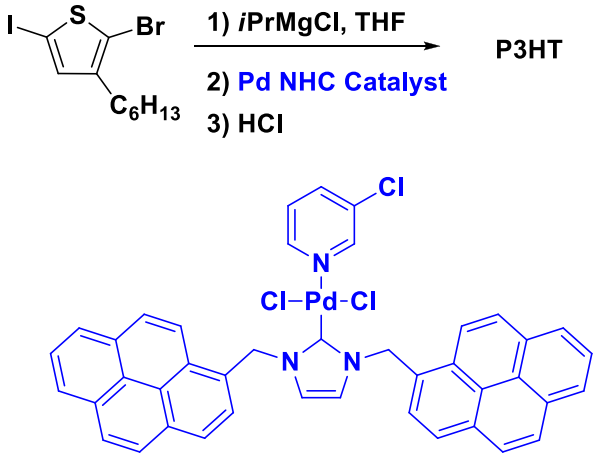

Figure 3.6. Synthesis of P3HT *via* KCTP initiated with Pd NHC catalyst **3**.

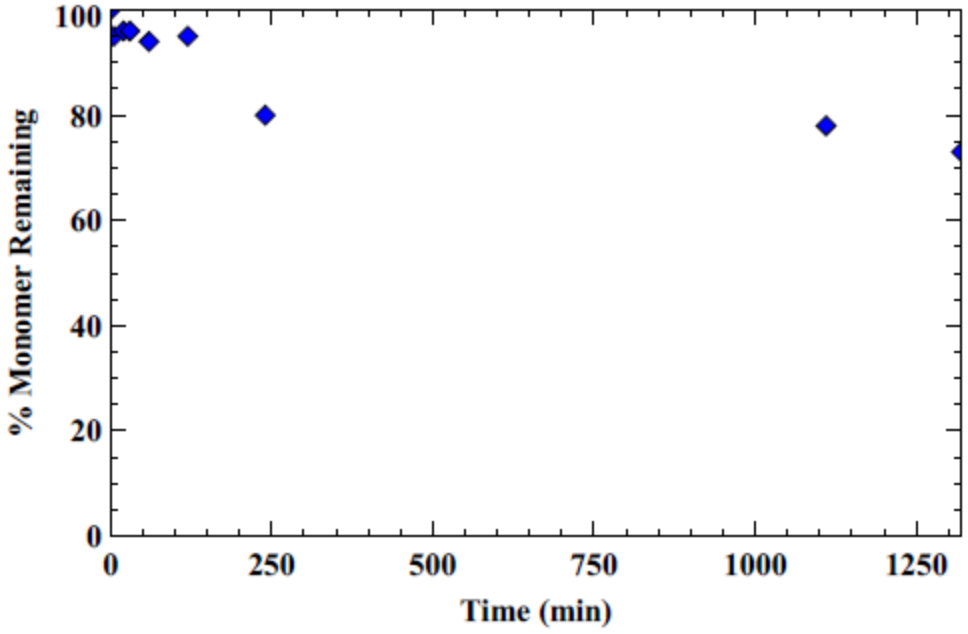

Figure 3.7. Percent monomer remaining *vs* time kinetics plot of KCTP initiated by catalyst **3**.

3.4 CONCLUSIONS

The small molecule Kumada Coupling model study with Pd NHC catalysts **1**-**3** exhibited very low reactivity compared to PEPPSI-IPr and Ni(dppp)Cl_2. NHC catalyst 3 displayed more intramolecular transfer products compared to catalysts **1** and **2** suggesting there may have been a benefit to having two π-conjugated ligands. However, the difference in ratios is not large and the effects from the ligands may be minimal. From this study, we can infer that catalysts **1**-**3** are not good candidates for CTP.

Chapter 4. INVESTIGATION OF BIMETALLIC NICKEL CATALYSTS BASED ON A TETRA(DIPHENYLPHOSPHANYLMETHYL)BENZENE DIAMINE LIGAND IN CATALYST-TRANSFER POLYMERIZATION OF Π-CONJUGATED POLYMERS

*The work in this chapter has been adapted from a previously published article: *Macromol. Chem. Phys.* **2019**, 1900363; doi: 10.1002/macp.201900363

4.1 INTRODUCTION

The previous studies with the NHC catalysts necessitated the need to rethink the approach in catalyst design for CTP. For the next study, catalysts were designed on emulating the structure of Ni(dppp)Cl_2 and the metal centers were spaced out farther. In this work, catalysts Ni_2(*m*-Ligand)Cl_4 and Ni_2(*p*-Ligand)Cl_4 were designed from a *N,N,N',N'*-tetra(diphenylphosphanylmethyl)benzene diamine ligand complexed to two Ni metal centers (**Figure 4.1**). The 1,3-benzene diamine ligand has been previously tested in Suzuki-Miyaura couplings where it has afforded enhanced catalytic rates with a variety of different aryl halide substrates.[57] The Suzuki couplings benefited from a stable association of the tetraphosphine 1,3-benzene diamine ligand with the Pd catalyst. Additionally, the benzene diamine ligand has been demonstrated to exhibit a balance of electronic and steric properties. For our own KCTP studies, the rigid aryl backbone could be advantageous for the stability of the metal π-aryl complex. The usage of the 1,4-benzene diamine ligand, a monometallic analogue based on aniline, and Ni(dppp)Cl_2 as a control allows us to understand the behavior of bimetallic complexes in CTP.

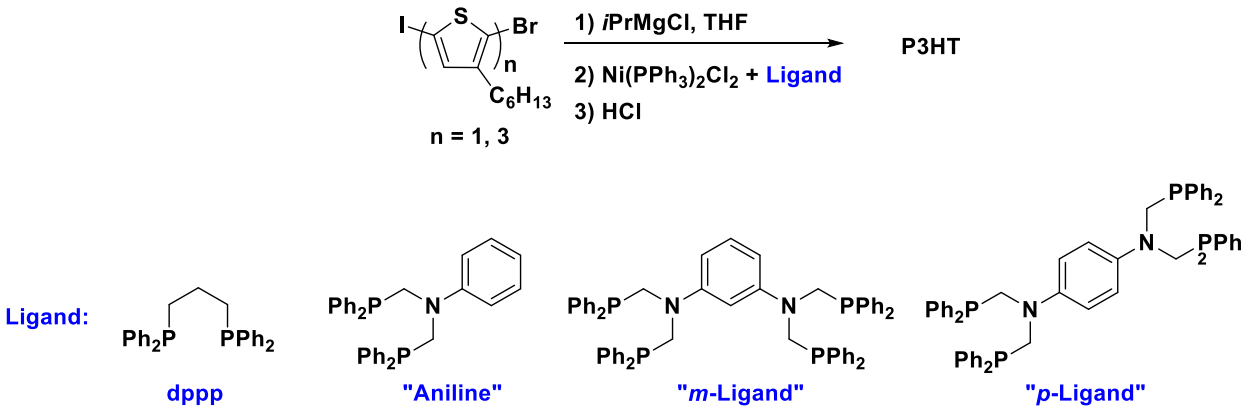

Figure 4.1. CTP mechanism showing the important metal-polymer π-complex.

A comparative study of the nickel catalysts is presented through kinetics that analyzed monomer conversion, degree of polymerization (DP), end-group functionalization and dispersity. To test if the length of the monomer would influence catalyst performance, 2-bromo-3-hexyl-5-iodothiophene "(3-HT)" and 5"-bromo-3,4',4"-trihexyl-5-iodo-[2,2';5',2"]terthiophene "$(3\text{-HT})_3$" were selected as the test monomers. Increased chain termination has been seen with terthiophene monomers,[18] however KCTP retained a relatively robust chain-growth mechanism due to the relatively stable metal π-aryl complex. For systems that do not share such a stable association, the length of distance between the catalyst and the next aryl halide bond may be detrimental to polymerization as it may stall or halt intramolecular oxidative addition.

4.2 EXPERIMENTAL

4.2.1 *Materials*

Reagents were obtained from commercial suppliers (Sigma-Aldrich, Fisher Scientific, ACROS, VWR, TCI) and unless noted, were used as received without further purification. Solvents were obtained from Pure Solv dry stills or redistilled before use. Reactions were carried out using Schlenk lines or in a glovebox under N_2 when necessary. All synthesized compounds

were purified through standard techniques, such as column chromatography, recrystallization, extraction, or filtration.

4.2.2 *Analytical characterization*

^{1}H-NMR and ^{31}P-NMR spectra in solution were recorded from Bruker 300 or 500 MHz AVance series instruments. End-groups of P3HT were identified using a Matrix-Assisted Laser Desorption/Ionization-Time of Flight MS (MALDI-TOF) Bruker Autoflex II instrument with a 337 nm laser and 2,2':5'2"-terthiophene as the solid matrix. Molecular weight distribution of polymers was determined using a Viscotek TDA 305 gel-permeation chromatography (GPC) coupled with an RI detector, multi-angle light scattering detector, and viscometer. Tetrahydrofuran was used as the eluent at 0.5 mL/min using conventional calibration of a narrow dispersity polystyrene standard. Single crystal X-ray analysis was collected at -173 ^{o}C on a Bruker APEX II single crystal X-ray diffractometer, using Mo-radiation. Crystals were mounted on a loop with oil before analysis.

4.2.3 *Theoretical calculations*

Using Gaussian 16 (version A03), Density Functional Theory (DFT) studies were performed on the bimetallic catalysts *via* the B3LYP functional. A hybrid basis set was deemed a necessity due to the presence of the Ni and Br atoms. The Ni and Br atoms required use of the LANL2DZ basis set while the remaining C, N, S and P atoms required use of the 6-31g* basis set. The pseudopotential for non-valence electrons were modeled using the LANL2DZ basis set as well. This work was facilitated though the use of advanced computational, storage, and networking infrastructure provided by the Hyak supercomputer system at the University of Washington.

4.2.4 *Synthesis of monomers and nickel catalysts*

Syntheses of $(3HT)_3$, phosphine ligands, and their precursors were based on previously reported procedures (**Figures 4.2 - 4.4**).[57–63] Synthesis and isolation of catalysts for characterization were carried out using $NiCl_2$ hexahydrate to simplify purification procedures.

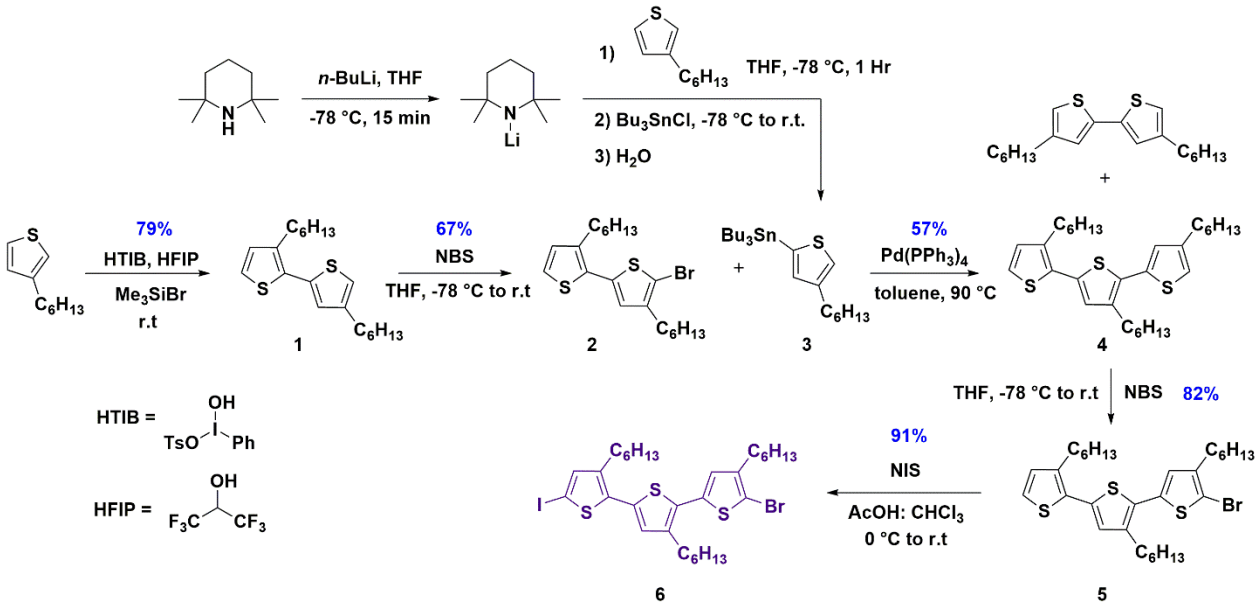

Figure 4.2. Synthesis of $(3\text{-HT})_3$ **6**.

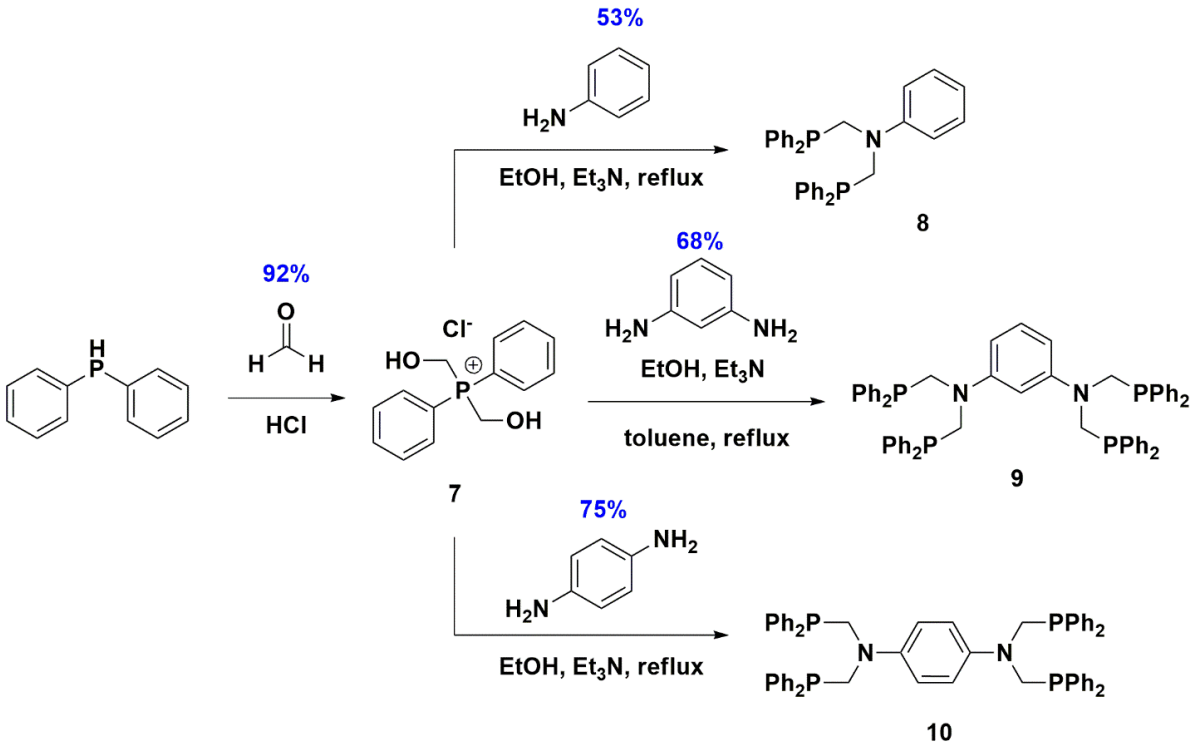

Figure 4.3. Synthesis of phosphine ligands.

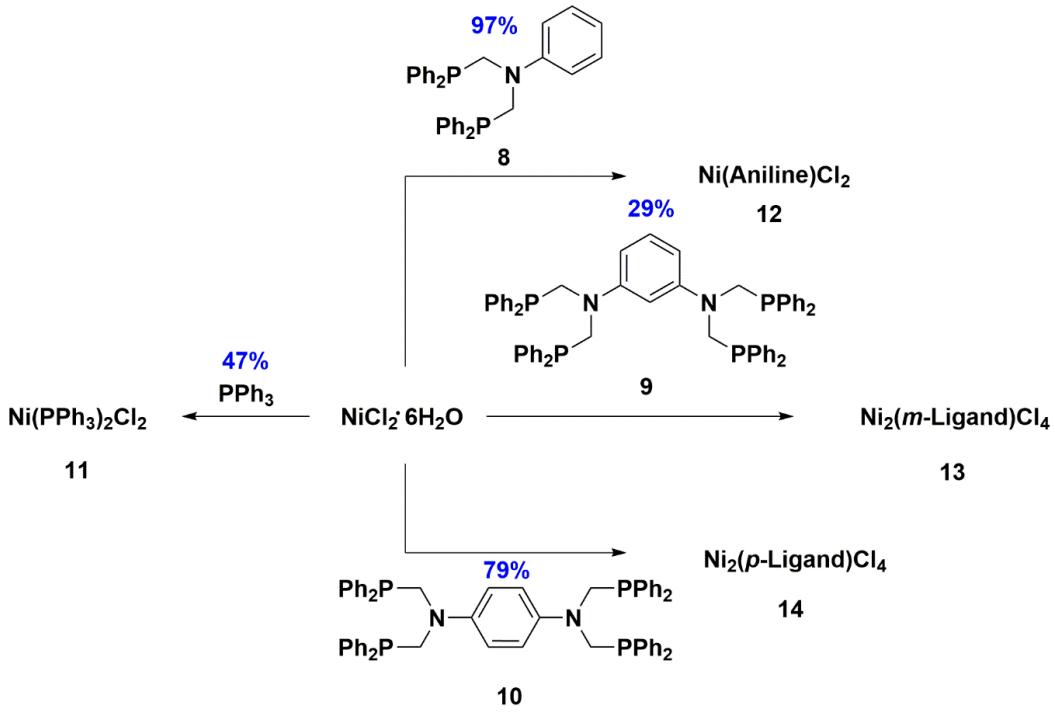

Figure 4.4. Synthesis of nickel catalysts.

4.2.5 *Synthesis of P3HT via KCTP*

The general experimental conditions for the polymerization of the (3-HT) monomer are described below: 2-bromo-3-hexyl-5-iodothiophene (0.22 mL, 1 mmol) was placed under high vacuum for several minutes and then purged with N_2. The reference standard, 1,3,5-trimethoxybenzene (8.4 mg, 0.05 mmol) was added and the reaction vessel was vacuum purged with N_2. Anhydrous tetrahydrofuran (10 mL) was added *via* syringe. While stirring, the reaction mixture was cooled to 0 °C. Isopropylmagnesium chloride (2.0 M in THF, 0.95 mmol) was slowly added dropwise *via* syringe. After removing the cooling bath, the reaction was warmed to room temperature to stir for an hour. $Ni(PPh_3)_2Cl_2$ (27.5 mg, 0.042 mmol) and ligand (0.042 mmol for monometallic reactions and 0.021 mmol for bimetallic reactions) were simultaneously added to the reaction mixture. The reaction was stirred at room temperature for three hours, then quenched with 1.5 mL of 2 M HCl. After 10 minutes, the mixture was added to a flask containing excess methanol resulting in the formation of precipitate. The solid was subsequently filtered and washed with methanol and then acetone until the filtrate solution was clear. The polymer was collected and dried in a vial *in-vacuo*.

The general experimental conditions for the polymerization with the $(3\text{-HT})_3$ monomer are nearly the same as the previously described procedures, but with these notable changes: 5"-bromo-3,4',4"-trihexyl-5-iodo-[2,2';5',2"]terthiophene (0.2329 g, 0.33 mmol) is reacted with isopropyl magnesium chloride (2.0 M in THF, 0.32 mmol). The polymerization was conducted at 0 °C and completed in one hour.

4.2.6 *Procedure for Ni catalyst kinetic studies of P3HT via ^{1}H-NMR*

Triplicate kinetic studies were carried out for polymerizations involving (3-HT) and (3-HT)$_3$ for each catalyst using the previously mentioned KCTP procedure where catalysts were generated *in-situ* upon addition into the reaction flask after the completion of the Grignard step. 1,3,5-trimethoxybenzene (8.4 mg, 0.05 mmol) was used as a reference standard and added before the Grignard step. Before the catalyst and ligand are added, a time 0 aliquot was removed from the reaction mixture. Upon initiating the polymerization, six to eight aliquots of 0.2 mL were removed from the reaction and added to a vial containing 1.0 mL of $CHCl_3$. Each aliquot was quenched with aq. HCl (3.0 M). 0.6 mL of the organic layer was extracted into a vial after drying through a filter containing Na_2SO_4. Solvent was evaporated *in-vacuo*. 0.6 mL of $CDCl_3$ was added to each vial and analyzed by ^{1}H-NMR. Calculation of predicted M_n is based on Equation (2) and (3) where n = number of repeating units; [M_i] = mmol of Grignard monomer and [Ni_i] = mmol of $Ni(PPh_3)_2Cl_2$.

$$n = \left(\frac{[M_i]}{[Ni_i]}\right) \tag{2}$$

$$M_{n(Predicted)} = n \times (M.W.of\ repeating\ unit) \tag{3}$$

4.3 Results and Discussion

4.3.1 *Synthesis and ICP-MS analysis of Ni Catalysts*

Synthesis of the Ni catalysts is shown in Figure 4.4. To ease the synthesis and purification, all three benzene amine ligands were reacted with $NiCl_2{\cdot}6H_2O$ instead of $Ni(PPh_3)_2Cl_2$ to avoid ligand substitution and release of PPh_3. ICP-MS was used to determine the purity of the catalysts by analyzing the Ni content. $NiCl_2{\cdot}6H_2O$ and Ni(dppp)Cl_2 samples from commercially available

supplies served as the controls for the experiment. **Table 4.1** summarizes the ICP-MS data of triplicate acid digestions in nitric acid. The relative purity for Ni(Aniline)Cl_2 and Ni_2(*p*-Ligand)Cl_4 was comparable to the Ni(dppp)Cl_2 analyte, based on the percent error from the theoretical Ni concentration. For Ni_2(*p*-Ligand)Cl_4, the observed Ni concentrations indicate that there is a mixture of bimetallic and monometallic complexes. A mixture of catalyst species can potentially contribute to a reduced CTP performance. Since we were unable to isolate and purify our pre-catalysts due to solubility issues, we conducted the polymerizations by generating the active catalyst *in-situ*.

Table 4.1. Reported ICP-MS data. Analysis of Ni content was completed using triplicates.

Entry	Catalyst	^{58}Ni (ppb)	^{60}Ni (ppb)	Mass (mg)	% Ni composition	Theoretical [Ni] (ppb)	% Error [^{60}Ni]
1	$NiCl_2 \cdot 6H_2O$	69.372	71.346	2.909	24.69	71.823	0.7
2	$NiCl_2 \cdot 6H_2O$	70.881	71.716				0.1
3	$NiCl_2 \cdot 6H_2O$	68.874	69.431				3.3
4	Ni(dppp)Cl_2	30.700	31.803	0.857	10.83	37.125	14.3
5	Ni(dppp)Cl_2	30.284	32.173				13.3
6	Ni(dppp)Cl_2	30.801	32.385				12.8
7	Ni(Aniline)Cl_2	28.883	30.550	0.935	9.48	35.455	13.8
8	Ni(Aniline)Cl_2	29.872	31.030				12.5
9	Ni(Aniline)Cl_2	29.630	31.232				11.9
10	Ni_2(*p*-Ligand)Cl_4	41.182	42.903	0.91	10.12	36.837	16.5
11	Ni_2(*p*-Ligand)Cl_4	40.143	42.065				14.2
12	Ni_2(*p*-Ligand)Cl_4	38.936	41.203				11.9
13	Ni_2(*m*-Ligand)Cl_4	19.156	19.757	0.862	10.12	34.894	43.4
14	Ni_2(*m*-Ligand)Cl_4	19.095	20.211				42.1
15	Ni_2(*m*-Ligand)Cl_4	17.495	18.910				45.8
16	Ni_2(*m*-Ligand)Cl_4	27.460	29.421	0.983	10.12	39.792	26.1
17	Ni_2(*m*-Ligand)Cl_4	27.088	28.053				29.5
18	Ni_2(*m*-Ligand)Cl_4	28.009	29.917				24.8

4.3.2 *^{1}H-NMR kinetic studies*

4.3.2.1 Comparison of monomer conversion rates

Monomer conversion provided useful insight into the catalyst performance in CTP and chain-growth behavior. The conversion of 2-bromo-5-chloromagnesio-3-hexylthiophene was monitored by comparing the ratio of the integration of its signal from its protonated form at the 5-position of the thiophene ring to the integration of the signal from the aromatic proton in 1,3,5-trimethoxybenzene, the internal standard (**Figure 4.5**). The disappearance of the thiophene proton doublet easily allowed the calculation of percent monomer remaining. **Figure 4.6** summarizes the kinetic studies on the polymerizations of (3-HT) and $(3\text{-HT})_3$. For the polymerization of (3-HT) (Figure 3a), monomer conversion rates were similar for all catalysts, except for at the 5-minute time point, where Ni(dppp)Cl_2 has a conversion 8 – 12 % higher than the other three catalysts demonstrating that it is still the most efficient catalyst for the synthesis of P3HT amongst the systems compared for this study. For polymerization of $(3\text{-HT})_3$ (Figure 3b), conversion rates were similar for all four catalysts; however, monomer conversion was low overall. This suggests the reaction is prematurely ending due to chain termination, which leads to short chain lengths of P3HT.

The kinetic trials suggest that no cooperative effects occurred between the two Ni metal centers and that they are acting as two independent sites. If the two metal centers were acting cooperatively, degree of polymerization (DP) will be affected. Specifically, we would expect DP to double for the bimetallic catalysts. This is not the case with the current findings. While it is unfortunate that the monometallic and bimetallic aminobenzene catalysts performed less efficiently than Ni(dppp)Cl_2, we rationalize that the electronic character and geometry are the primary causes, as will be discussed below.

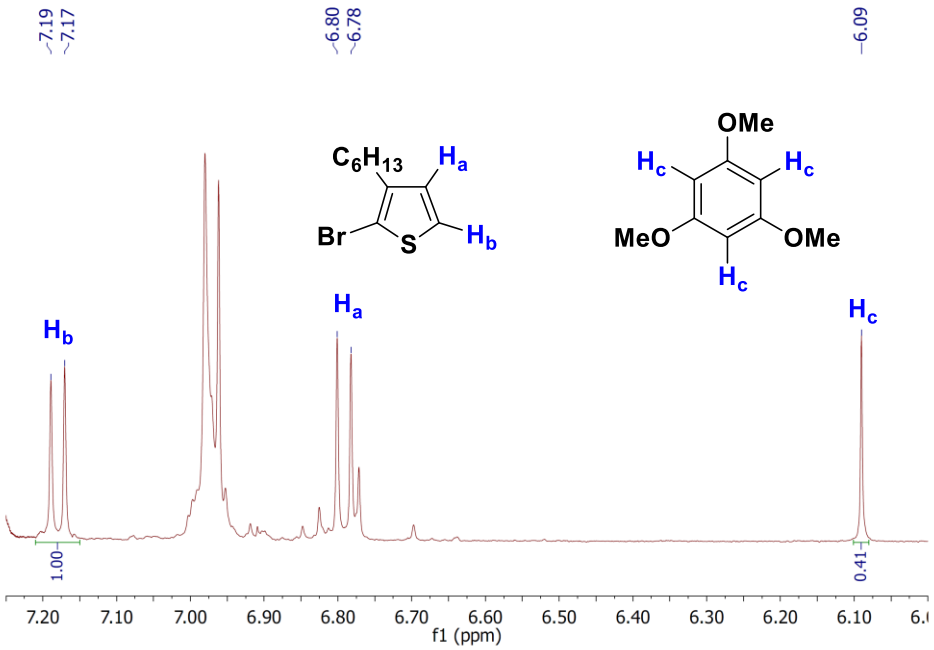

Figure 4.5. ^{1}H-NMR ($CDCl_3$) of mixture containing P3HT, unreacted monomer (2-bromo-3-hexylthiophene) and 1,3,5-trimethoxybenzene reference.

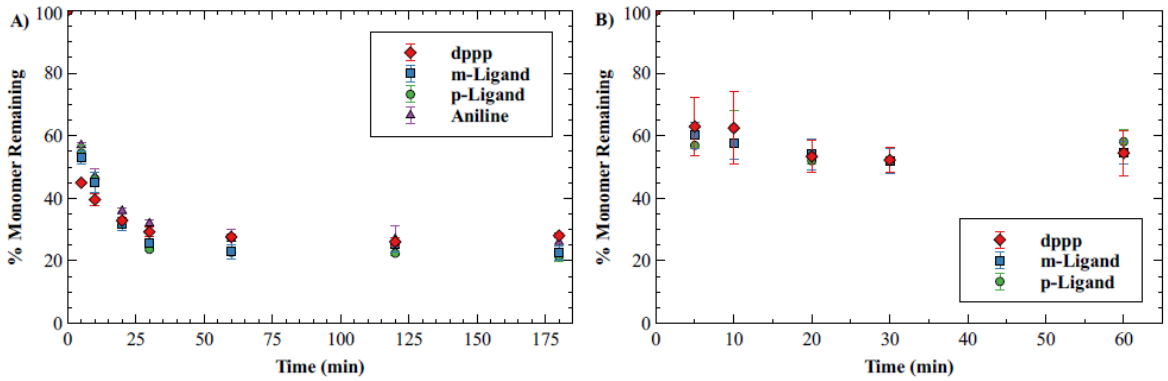

Figure 4.6. Percent monomer remaining *vs.* time plot of (3-HT) (A) and $(3\text{-HT})_3$ (B) kinetic trials with error bars showing standard deviation.

4.3.2.2 Analysis of molecular weight and degree of polymerization via ^{1}H-NMR

Based on the kinetics data, we hypothesized the Ni metal sites of the catalysts are behaving independently of each other. We rationalize this by looking at M_n of the isolated polymers. If the two metal centers are independently active and growing two separate polymers, then the degree of

polymerization should equal the ratio of [M_i] over [Ni_i] as seen in Equation (2). If the two metal centers were cooperatively active and only bound to one polymer, then DP should double, since M_n is a function of the molar ratio of monomer to the catalyst. Lower catalyst concentrations results in an increase in DP.[64]

To determine DP, ^{1}H-NMR was used to analyze the region that contained the α-methylene protons on the hexyl side chain of P3HT (**Figure 4.7)**.[65] Using Equation (1), DP can be determined by comparing the integration ratio between the α-methylene protons belonging to the repeating head-to-tail (H-T) coupled thiophene rings to the tail-to-tail (T-T) regioisomer, and chain-end thiophene rings. The α-methylene protons of the dominant repeating H-T thiophenes are located at 2.65 – 2.9 ppm and the integration signals at 2.5 – 2.65 ppm represent the α-methylene protons that belong to the T-T regioisomer and chain-end rings (Figure 4.7). By setting the integration of the α-methylene protons (H_b – H_e) equal to two, the integration of H_a plus two to accommodate the end-group thiophene units equals DP.[50]

$$DP = \left(\frac{I_{repeating\ unit}}{\#\ of\ protons\ of\ repeating\ unit} \times \frac{\#\ of\ protons\ of\ end-groups}{I_{end-groups\ and\ regioisomers}}\right) + 2 \quad (1)$$

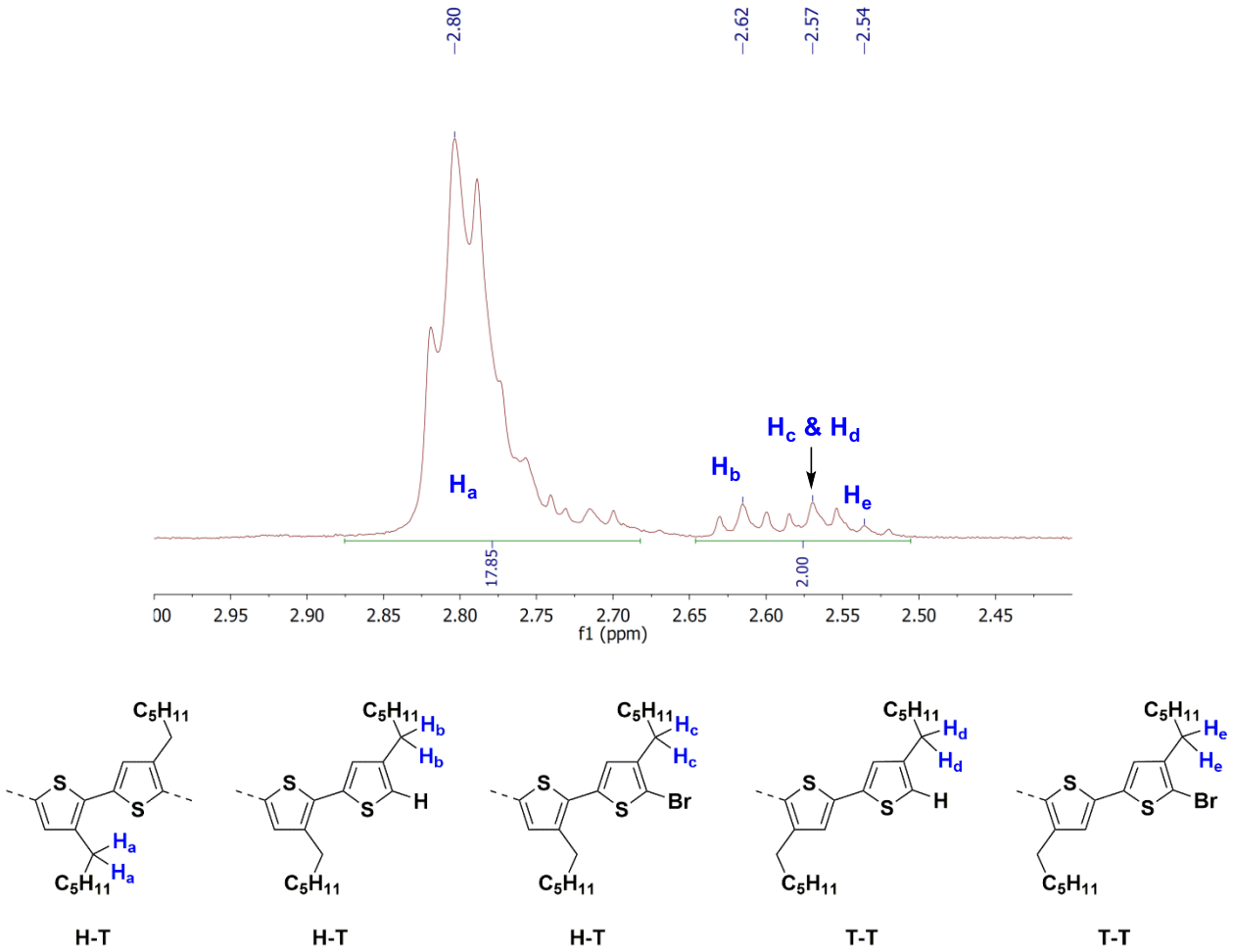

Figure 4.7. ^{1}H-NMR of the methylene protons on the hexyl chain of P3HT regioisomers.

Table 4.2 and **4.3** summarize the M_n and DP calculated from monomer conversion in the (3-HT) and $(3\text{-HT})_3$ polymerizations, respectively. In Table 1, the range of DP for the (3-HT) trials (Entries 1-12) is between 15 and 22 while for the $(3\text{-HT})_3$ polymerizations, the range was three to four. Entries 7-12 and 14 of Table 4.2 and entries 4-9 of Table 4.3 display two columns of predicted M_n values that result from having either one or two polymer chains growing for the bimetallic catalysts. For these entries, we found that actual M_n aligned with the predicted M_n where two separate polymers are growing on each Ni active site, thus supporting the hypothesis that the metal centers are acting independent of each other. While the two metal centers are not interacting with the same polymer, the successful synthesis of P3HT with the three diphenylphosphanylmethyl

benzene amine catalysts is promising. Further studies in the employment of cooperative bimetallic catalysts is needed ensure only one polymer is bound in the Ni(0) polymer π-complex.

Table 4.2. Results of (3-HT) polymerization trials.

Entry	Ligand	Monomer Conversion (%)	Predicted M_n (kg/mol)[a)]	Predicted M_n (kg/mol)[b)]	Actual M_n (kg/mol)	DP	$Đ$	Yield (%)[c)]
1	Dppp	76	3.3	-	3.0	20	1.22	71
2	Dppp	73	3.2	-	3.2	19	1.24	66
3	Dppp	74	2.8	-	2.9	17	1.28	66
4	Aniline	68	2.0	-	2.5	15	1.74	52
5	Aniline	79	3.3	-	3.3	20	1.95	75
6	Aniline	77	3.4	-	3.2	20	1.87	74
7	*m*-Ligand	76	3.3	5.8	3.3	22	1.85	74
8	*m*-Ligand	83	3.6	6.2	3.5	21	1.69	67
9	*m*-Ligand	74	2.4	5.6	3.2	19	1.56	50
10	*p*-Ligand	77	3.3	5.8	2.7	16	2.10	76
11	*p*-Ligand	81	3.4	6.2	3.2	20	1.83	78
12	*p*-Ligand	79	3.5	6.0	3.5	21	1.55	61
13	Dppp	78	5.9	-	5.3	32	1.33	79
14	*m*-Ligand	81	6.2	12.0	3.7	22	1.83	70
15[d)]	*m*-Ligand	-	-	-	4.2	25	1.84	78
16[d)]	*p*-Ligand	-	-	-	4.0	24	1.96	52

a) M_n (Predicted) is based on two polymer chains growing on bimetallic catalysts; **b)** M_n (Predicted) is based on one chain growing on bimetallic catalysts; **c)** Isolated polymer was obtained after purification with methanol and acetone washes; **d)** Entries 15 and 16 were ran to completion with no aliquots taken with the intention of just viewing the DP of isolated P3HT.

Table 4.3. Results of $(3\text{-HT})_3$ polymerization trials.

Entry	Ligand	Monomer Conversion (%)	Predicted M_n (kg/mol)[a)]	Predicted M_n (kg/mol)[b)]	Actual M_n (kg/mol)	DP	$Đ$	Yield (%)[c)]
1	Dppp	39	2.4	-	1.5	3	1.32	23
2	Dppp	58	3.2	-	2.2	4	1.29	49
3	Dppp	51	2.3	-	1.8	4	1.40	36
4	*m*-Ligand	39	3.1	6.2	1.8	4	1.31	34
5	*m*-Ligand	51	3.4	6.8	1.5	3	1.36	34
6	*m*-Ligand	56	3.1	6.2	1.9	4	1.50	49
7	*p*-Ligand	56	3.4	6.8	1.4	3	1.33	25
8	*p*-Ligand	46	2.6	5.2	1.7	3	1.44	39
9	*p*-Ligand	49	2.5	5.0	1.9	4	1.56	36

a) M_n (Predicted) is based on two polymer chains growing on bimetallic catalysts; **b)** M_n (Predicted) is based on one chain growing on bimetallic catalysts; **c)** Isolated polymer was obtained after purification with methanol and acetone washes.

Entries 13-16 of Table 4.2 are the results of polymerizations of (3-HT), where a DP of 48 was targeted. To increase DP to 48, the catalyst loading was halved. Entry 13 served as a control reaction with $Ni(dppp)Cl_2$ while entries 14-16 represent reactions completed with the bimetallic catalysts. Interestingly, P3HT obtained from KCTP initiation with the bimetallic catalysts (Entries 14-16) did not have increased M_n values in the same manner as the control (Entry 13). This was an unexpected result, since the previous kinetics studies showed the catalysts performed similarly. We suspect the limitation in M_n to be caused by early chain termination; steric hindrance in the bimetallic catalyst geometry may be making it difficult for longer chains to form. This may interfere with the integrity of the metal π-aryl complex where, upon polymer dissociation, the metal center is free to initiate a new chain.

The M_n values obtained for the $(3\text{-HT})_3$ polymerizations (Table 4.3) provide further support for two polymer chains growing on the bimetallic catalysts (Entries 4-9). The observed low M_n when compared to the predicted calculations suggests KCTP is prematurely terminating. Chain termination in KCTP, which indicates a reduction in control over the polymerization, is not ideal for the synthesis of π-conjugated polymers when desired and precise M_n values are being targeted.

A possible source for this chain termination can be attributed to Ni(0) dissociation,[41] which can occur due to the stalling of oxidative addition. Another possible factor is the steric hinderance of a larger monomer, as described above. This crowding of the Ni coordination sphere with (3-HT) is smaller compared to $(3\text{-HT})_3$ and affects different parts of KCTP: the rate of reductive elimination will increase, but the rate of transmetalation will be decrease.

4.3.3 *Analysis of CTP behavior*

4.3.3.1 End-group identification using MALDI-TOF MS

The success of controlled CTP relies on a stable metal π-aryl complex. Deviations from the ideally controlled polymerization can be observed by looking at end-group content and dispersity. To gain insight on the extent of chain termination, end-group analysis was conducted with MALDI-TOF MS. A controlled polymerization would show P3HT with only Br/H chain ends. The presence of P3HT with Br/Br end-groups indicate interchain termination or catalyst dissociation.[66] **Figure 4.8** illustrates the pathways that can result in P3HT containing H/Br or Br/Br end-groups. The release of the catalyst through either dissociation or disproportionation can cause another initiated cycle of KCTP resulting in the decrease in uniformity of polymer chains and higher dispersity.

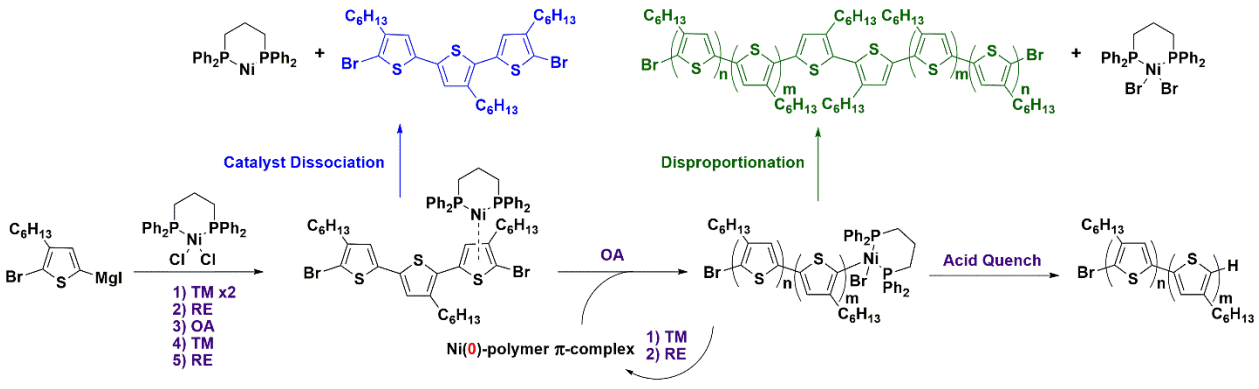

Figure 4.8. General reaction cycle of KCTP showing the ideal pathway (below) and the unideal pathways that result in chain termination (above).

Figure 4.9 represents the MALDI-TOF data obtained from the polymerizations conducted on (3-HT) while **Figure 4.10** displays the MALDI-TOF data for the $(3\text{-HT})_3$ polymerizations. Upon analyzing the end-groups of the polymers, Br/Br end-group content was shown to increase in the following order: Ni(dppp)Cl_2 < Ni(Aniline)Cl_2 = Ni_2(*p*-Ligand)Cl_4 < Ni_2(*m*-Ligand)Cl_4 for the (3-HT) trials. Ni(dppp)Cl_2 was expected to show majority H/Br end-groups, since it is known for its high performance in exhibiting molecular weight control in KCTP. Analysis of P3HT synthesized through KCTP initiated by Ni(Aniline)Cl_2 (Figure 4.9c) showed end-group content similar to Ni_2(*p*-Ligand)Cl_4 (Figure 4.9b). This result is consistent with our earlier observations, as we believe Ni_2(*p*-Ligand)Cl_4 exhibits similar catalytic behavior to Ni(Aniline)Cl_2 since the metal sites are acting independent of one another. The coordination sites are oriented in opposite directions, mitigating steric interactions between the two growing polymer chains. The relatively high content of Br/Br in Ni_2(*m*-Ligand)Cl_4 (Figure 4.9d) is likely linked to the catalyst geometry. Compared to the other catalysts, the coordination sphere of Ni_2(*m*-Ligand)Cl_4 is very crowded, especially for the case of having two different polymer chains growing on the same molecule. Sterics from either the monomer[67] or catalyst structure[21] have been shown to influence the rate of polymerization. The sterically crowded coordination sphere is potentially facilitating the collapse of the Ni(0) π-aryl complex, releasing the polymer before oxidative addition can occur. When comparing the end-group content observed with Ni_2(*p*-Ligand)Cl_4 and Ni(Aniline)Cl_2 to Ni(dppp)Cl_2 (Figure 4.9a), it appears that sterics cannot be the primary source for increased Br/Br content, because the coordination spheres are not crowded. We suspect the difference between end-group content to be related to the electronic structure of the benzene amine ligand. While the coordination sites of Ni(Aniline)Cl_2, Ni_2(p-Ligand)Cl_4, Ni_2(*m*-Ligand)Cl_4 emulated Ni(dppp)Cl_2

in structure, the presence of the benzene amino moiety may be affecting the stability of the metal π-aryl complex.

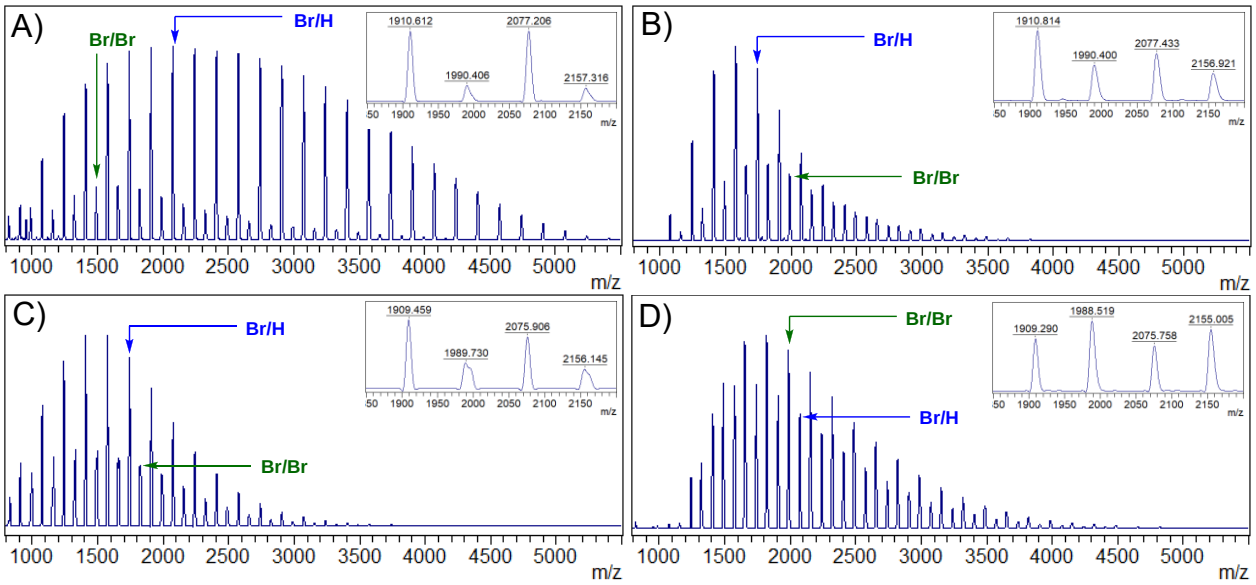

Figure 4.9. MALDI-TOF data for (3-HT) KCTP polymerization. (A) Ni(dppp)Cl_2; (B) Ni(Aniline)Cl_2; (C) Ni_2(*p*-Ligand)Cl_4; (D) Ni_2(*m*-Ligand)Cl_4

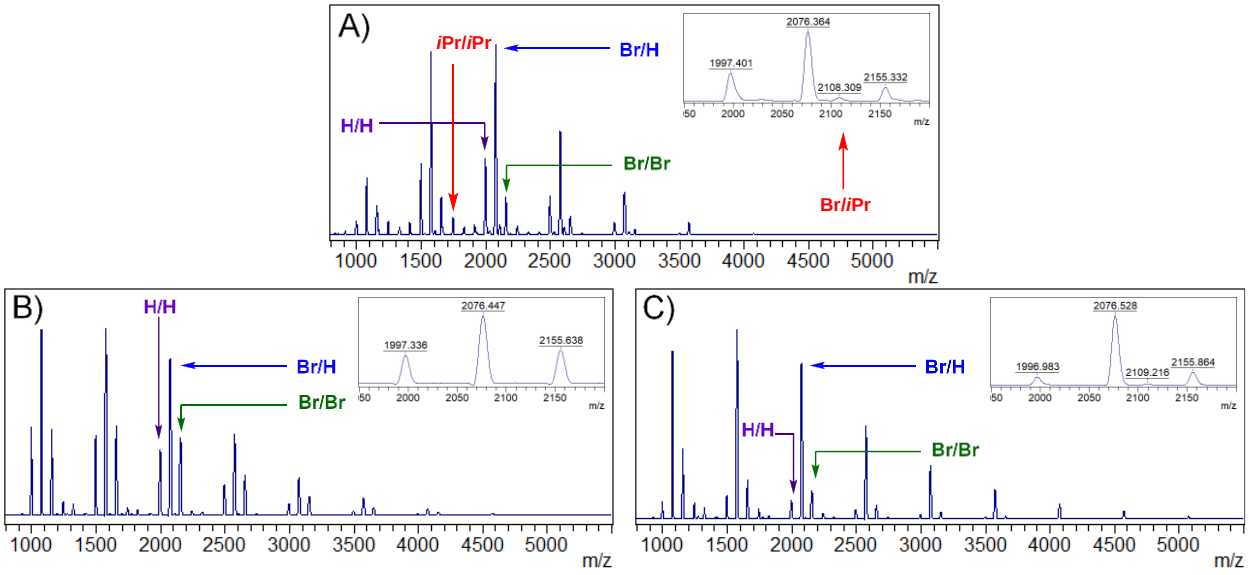

Figure 4.10. MALDI-TOF data for $(3\text{-HT})_3$ KCTP polymerization. (A) Ni(dppp)Cl_2; (B) Ni_2(*p*-Ligand)Cl_4; (C) Ni_2(*m*-Ligand)Cl_4

While sterics appears to be playing a contributing factor in the reduced controlled polymerizations, we cannot ignore the possibility that electronics also has a role in affecting catalyst performance. As mentioned before with the Suzuki couplings,[57] the 1,3-benzene diamine ligand was hypothesized to form a stable association with the Pd catalyst. While a stable metal π-aryl complex is needed for controlled KCTP, too strong of an association is detrimental as it will prevent oxidative insertion from occurring. This is due to the Ni(0) catalyst remaining adhered to the polymer chain preventing "ring-walking" from occurring. Very stable metal π-aryl complexes have been observed with polymerizations of thiophene-benzothiadiazole-thiophene, thienothiophenes, and *p*-phenylene vinylene monomers.[31,34,36,68] The ligand to metal donation of the benzene amino ligand may be weaker if the aniline moiety is not donating electron density towards the phosphine group. The lack of electron donation between the ancillary phosphine ligand and the transition metal can destabilize the metal π-aryl complex. The structure of Ni(Aniline)Cl_2 will be explored later.

Disparity in end-group content with the $(3\text{-HT})_3$ polymerizations is not as pronounced, compared to the (3-HT) trials. In the $(3\text{-HT})_3$ polymerizations, H/H end-groups have been observed. Formation of H/H endcapped P3HT can result when excess Grignard reagent is added and both halides are exchanged. This is apparent when looking at the conversion for the Grignard formation *via* NMR and we find signals that represent the H-capped monomer. However, even when excess addition of Grignard reagent was mitigated, H/H end-groups still formed despite no apparent signals of H/H end-capped $(3\text{-HT})_3$ being present in the t = 0 aliquot. We suspect that this is due to incomplete active Grignard monomer formation. Additionally, the more electron rich $(3\text{-HT})_3$ may slow down the rate of magnesium-halogen exchange and affecting the ratios of H/H and H/Br end-groups. Evidence for unreacted Grignard species present in the reaction mixture is shown

in Figure 4.5 where the peaks representing P3HT endcapped with Br/*i*Pr and *i*Pr/*i*Pr are marked. For polymerizations that minimized H/H formation, H/Br end-group content was consistently higher than Br/Br for all three catalysts. This observation indicates that oxidative insertion is occurring, however transmetalation with the monomer is not occurring. Polymerization is most likely halted due to the larger size of the $(3\text{-HT})_3$, which can slow down transmetalation. The kinetics of the $(3\text{-HT})_3$ polymerization support the occurrence of premature termination, since a low M_n was observed for all three catalysts. After three to four couplings were achieved, subsequent transmetalations after oxidative addition of the Ni(0) π-aryl complex are exceedingly harder to occur, due to increased sterics from $(3\text{-HT})_3$. The presence of polymers with a higher content of non-ideal end-groups indicates a reduced controlled polymerization and leads to increased chain termination.[8] As a consequence, this results in a broader distribution of polymers with different molecular weights. Large batch-to-batch differences in polymer is undesirable since their physical and electronic properties can be affected.[69]

4.3.3.2 Chain-growth analysis and dispersity

Chain-growth behavior provides additional insight into the quality of the polymerization, and it can be determined by looking for a linear progression in M_n vs % monomer conversion. The kinetics from the (3-HT) polymerizations (Figure 4.2a) show an increase in M_n as monomer is converted over the three hours reaction time. For the $(3\text{-HT})_3$ polymerizations (Figure 4.2b), increase in M_n growth is difficult to observe, since the polymer stops growing after three or four couplings have occurred. Monomer conversion plateaued after 20 minutes have elapsed. To better understand the polymer distribution between the catalysts, we characterized the polymers obtained from the different time aliquots during the kinetic experiments using size-exclusion chromatography (SEC).

SEC provides a convenient analysis in understanding and predicting polymer performance by characterizing the molecular weight distribution of P3HT. Summary of SEC analyses is illustrated in Table 1 and 2 for the isolated polymers and **Figure 4.11** for the polymerization kinetics of (3-HT) and **Figure 4.12** for $(3\text{-HT})_3$. As expected, polymerizations completed with $Ni(dppp)Cl_2$ showed a linear relationship, indicating chain-growth behavior, and dispersity was low throughout the duration of the reaction (Figure 7a). $Ni(Aniline)Cl_2$, $Ni_2(p\text{-Ligand})Cl_4$, and $Ni_2(m\text{-Ligand})Cl_4$ all exhibit chain-growth, however dispersity values over the course of the reaction also increased linearly. The increased dispersity with $Ni(Aniline)Cl_2$, $Ni_2(p\text{-Ligand})Cl_4$, and $Ni_2(m\text{-Ligand})Cl_4$ aligns with the observed values obtained from the isolated polymers (Table 1). SEC analysis provides further evidence supporting the notion that the catalysts generated from the benzene amine ligands exhibit a reduced controlled polymerization compared to $Ni(dppp)Cl_2$.

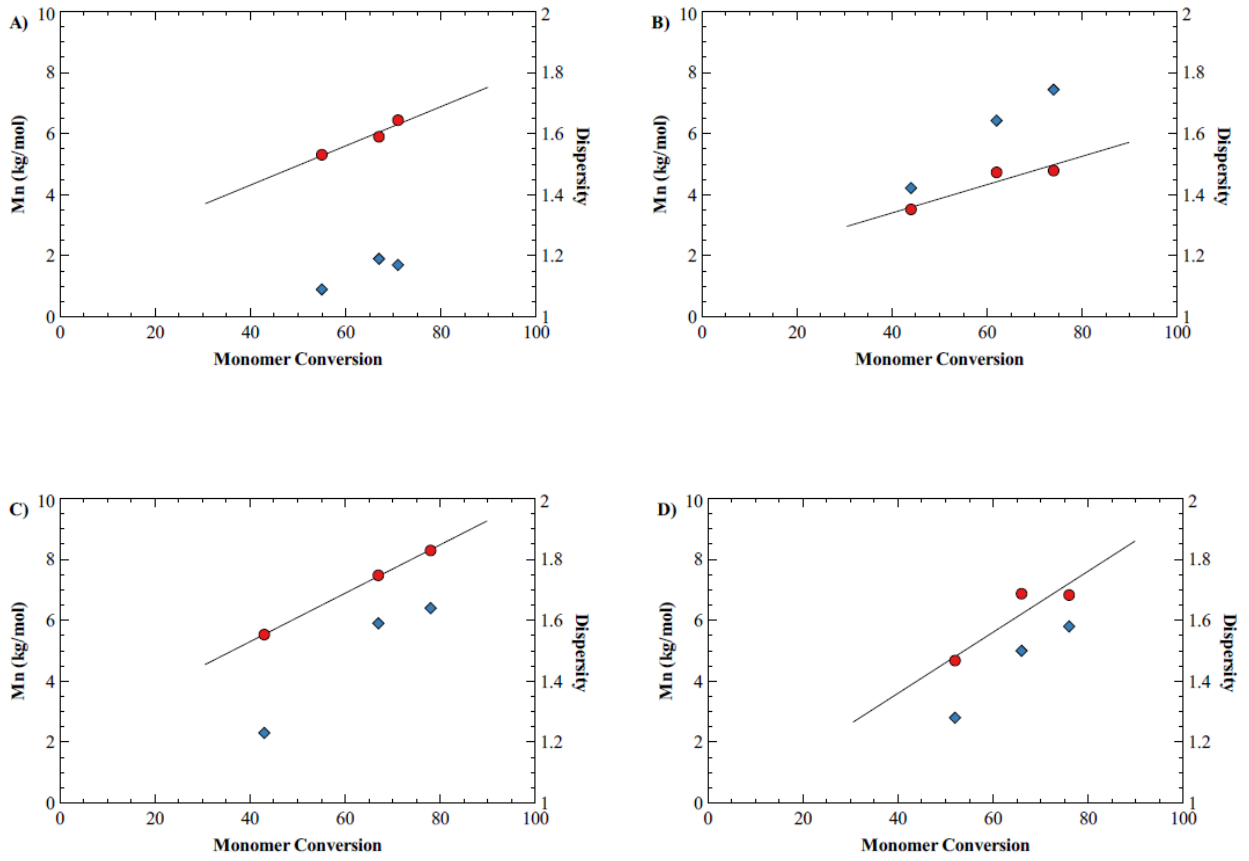

Figure 4.11. M_n versus monomer conversion for (3-HT) polymerizations (red circle). (A) Ni(dppp)Cl_2; (B) Ni(Aniline)Cl_2; (C) Ni_2(*p*-Ligand)Cl_4; (D) Ni_2(*m*-Ligand)Cl_4. Dispersity values over the course of the reaction are represented by blue diamonds.

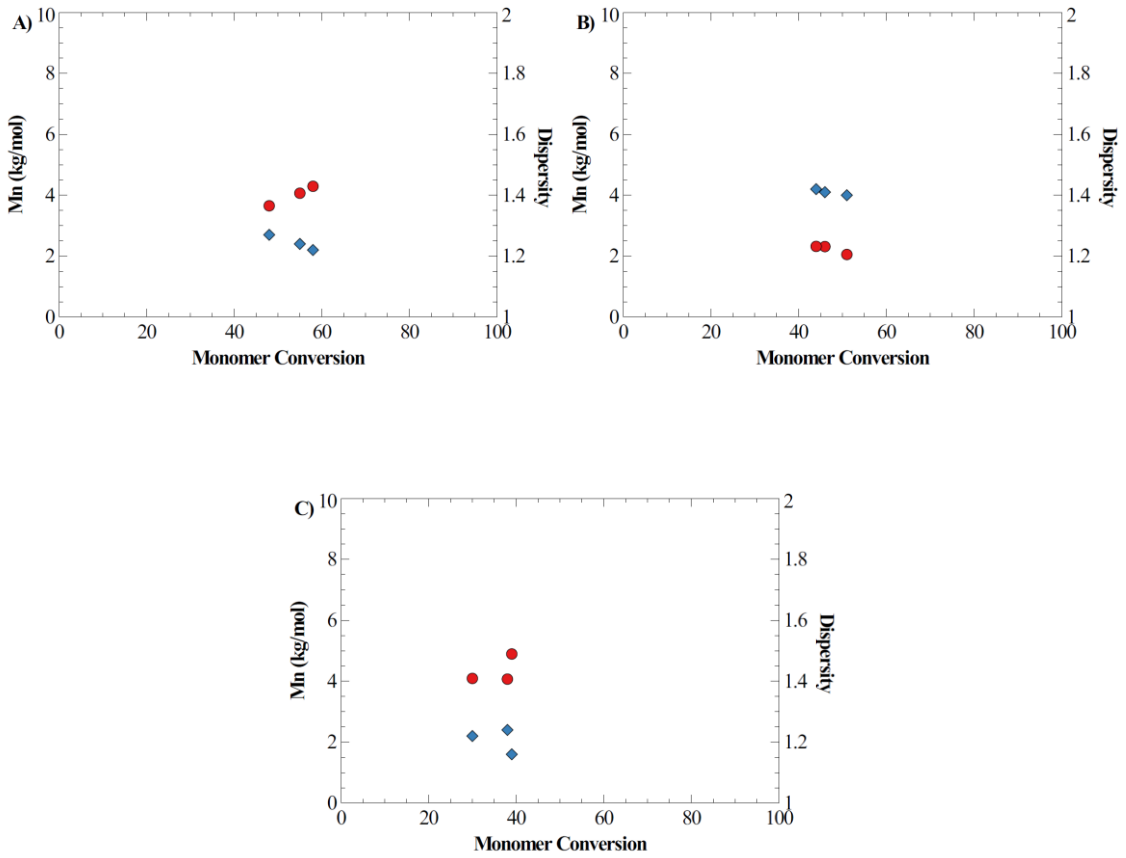

Figure 4.12. M_n versus monomer conversion for $(3\text{-HT})_3$ polymerizations (red circle). A) Ni(dppp)Cl_2; B) Ni_2(*p*-Ligand)Cl_4; C) Ni_2(*m*-Ligand)Cl_4.

4.3.4 *Characterization of Ni catalysts*

4.3.4.1 DFT Studies

Dispersity from SEC together with the increased in Br/Br terminated P3HT from MALDI analysis indicate a reduced controlled polymerization. The reported observations support the probability that premature chain termination is occurring. We suspected the Ni(0) π-aryl complex is not as stable with the benzene amine catalysts. With these findings, analysis of the catalysts was carried out *via* DFT studies to provide more insight on the structure of the bimetallic catalysts and to clarify the experimental observations.

DFT studies were completed on Ni_2(*p*-Ligand)Cl_4 and Ni_2(*m*-Ligand)Cl_4. Obtained datasets were modeled on the Ni(0) π-aryl complex bound to a terthiophene framework, with the alkyl group truncated for ease of calculations (**Figure 4.13**). The distance between the two Ni sites is 13.1 Å for the optimized structure of the Ni_2(*p*-Ligand) π-aryl complex and the metal centers are oriented in opposite directions. The large distance and direction the metal centers face most likely explains why the Ni metal centers behave independently of each other. They are too far apart to have any noticeable metal-to-metal proximity effect on the polymerization. The optimization of Ni_2(*m*-Ligand) π-aryl complex revealed a Ni-Ni distance of 11.3 Å. The bidentate ligands are oriented in a manner that minimizes the steric clash between the triphenylphosphine ligands. The optimized geometry of Ni_2(*m*-Ligand) π-aryl complex from DFT showed crowded metal sites, which suggest that steric interactions are playing a role in affecting CTP performance. This provides insight as to why there is increased Br/Br end-group formation with the (3-HT) polymerization.

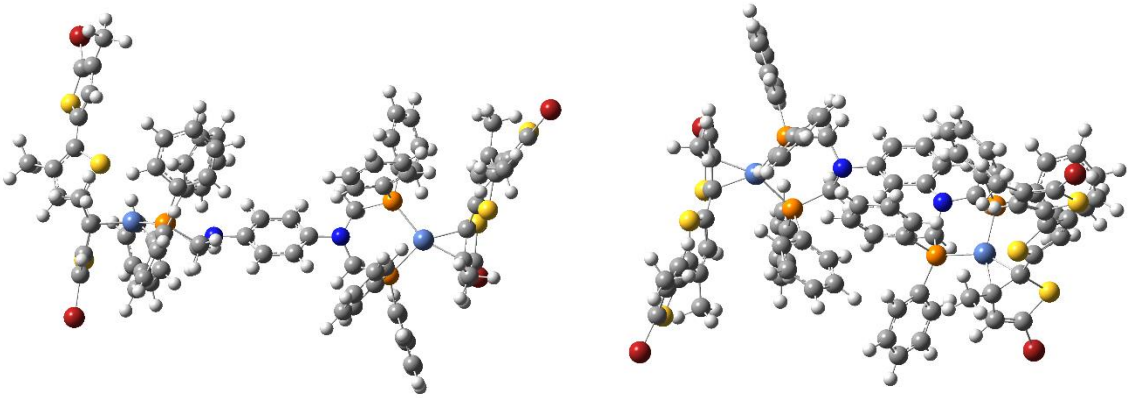

Figure 4.13. DFT optimized structures of Ni_2(*p*-Ligand) (left structure) and Ni_2(*m*-Ligand) (right structure) π-aryl complexes. Heteroatom identifications: Ni (light blue); Br (Red); N (Blue); P (Orange); S (Yellow).

4.3.4.2 X-ray crystallography of Ni(Aniline)Cl_2

Attempts to obtain high quality single crystals for X-ray analysis were successful only for the Ni(Aniline)Cl_2 catalyst. Crystals could not be obtained from Ni_2(*p*-Ligand)Cl_4 due to insolubility. For Ni_2(*m*-Ligand)Cl_4, spherulitic crystals were isolated, but were not suitable for analysis. Failure to obtain quality crystals is not surprising, as the *meta*-disubstituted bridged ligand may not be able to arrange in a highly ordered microscopic structure due to its geometry. The structure of Ni(Aniline)Cl_2 is shown in **Figure 4.14**. From the crystal structure, the reported bite angle of Ni(Aniline)Cl_2 is 94.89°. This angle is approximately 3 degrees larger than dppp, which is 91.77°.[70] We can infer from the increase in bite angle, that the cone angle of Ni(Aniline)Cl_2 will be larger than dppp (142°).[71]

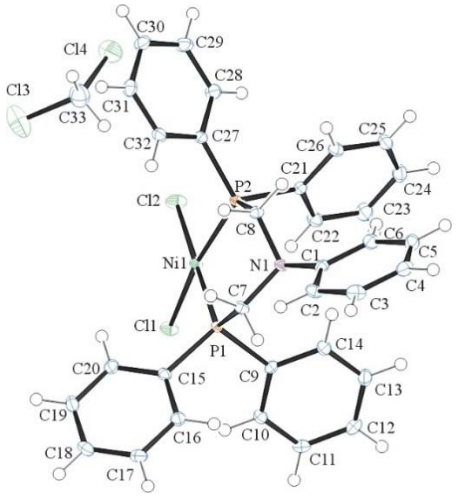

Figure 4.14. ORTEP of Ni(Aniline)Cl_2 with thermal ellipsoids at the 50% probability level.

From the crystal structure, we conclude that the metal π-aryl complex for the benzene diamine catalysts is weaker compared to Ni(dppp)Cl_2 due to the increased cone angle of the ligand. Ligand steric properties in CTP exhibit a “goldilocks” effect where a too large or too small cone angle is detrimental to CTP performance leading to unproductive pathways (i.e. chain termination).[7,18] The structure of Ni(dppp)Cl_2 can be viewed as the optimized geometry for the controlled synthesis of P3HT. By deviating from that geometry with a larger cone angle, the CTP

performance is reduced. The slight increase in bite and cone angles is enough to significantly alter the stability of the metal π-aryl complex. For Ni_2(*m*-Ligand)Cl_4, we imagine the cone angle is significantly larger compared to the other catalysts due to its inherent geometry. The finding from the crystal structure of Ni(Aniline)Cl_2 supports the distribution of Br/Br end-group between all four studied catalysts. Previously, the electronic character of the benzene diamine ligand was speculated to be playing a role in the increased Br/Br end-group content with Ni(Aniline)Cl_2 and Ni(*p*-Ligand)Cl_4 compared to Ni(dppp)Cl_2. We cannot rule out the difference in electronic character between the benzene amine and dppp in having an impact over the metal π-aryl complex stability. Reducing the electronic character of the ancillary phosphine ligand can slow down oxidative addition and increase the likelihood of chain transfer, thus worsening CTP. Further studies will be required to address the difference in electronic properties between the ancillary ligands.

4.4 CONCLUSIONS

A comparative polymerization to synthesize P3HT was developed to study the behavior of multi-catalysis in CTP. Ni catalysts constructed from a functionalized aminobenzene framework exhibited chain-growth behavior in KCTP. All catalysts displayed similar findings in M_n and monomer conversation rates. These observations indicate that two polymer chains are growing independently of one another on the two metal centers in the bimetallic catalysts. Additional kinetic studies have led to the observation that the polymerization of (3-HT) with the bimetallic catalysts have difficulty going beyond a chain length of DP = 25. This is a result of increased sterics in geometry of the benzene amine catalysts, which were seen to exhibit critical influence on the polymerization. While the synthesized catalysts emulated the structure of Ni(dppp)Cl_2, they do not perform as efficiently, resulting in reduced controlled polymerization in CTP. The poorer

CTP performance is attributed to a weaker Ni(0) π-aryl complex, leading to increased chain-termination in KCTP.

Broadening the scope of ligands is desirable in expanding KCTP with multi-catalysis. In addition to the influence of the monomer, the key steps in KCTP are heavily affected by choice of the ancillary ligands and reactive ligands of the catalyst initiator. Determining the ideal reaction conditions and compatibility between the catalyst and monomer is crucial in achieving controlled polymerization of π-conjugated polymers. More testing is needed to explore the applicability multi-catalysis in the synthesis of π-conjugated polymers. These initial experiments have provided promising insight into what structural features are desirable when designing a multimetallic catalyst that will exhibit controlled polymer chain-growth. Further investigations into bimetallic catalyst using a preorganized geometry are underway.

Chapter 5. INVESTIGATION OF A BIMETALLIC NICKEL CATALYSTS BASED ON A XANTHENE CORE LIGAND TO ORIENT THE METAL CENTERS IN THE SAME DIRECTION

5.1 INTRODUCTION

Catalyst transfer polymerization (CTP) has advanced the field of conjugated polymer synthesis by affording a variety of different architectures. However, the field has been stunted by disparity in monomer and catalyst compatibility. While improvements to CTP have focused on fine tuning the ancillary ligands, reactive ligands and transition metal of the catalyst, compatibility with monomers remains an issue. CTP has been primarily successful with simple and electron-rich monomers. For monomers that comprised of electron-deficient units, successful and controlled polymerizations are scarce.

To further the synthesis of conjugated polymers with CTP, further understanding of monomer-catalyst interactions is important. In CTP, it is known that its controlled behavior is connected to the highly suspected existence of a metal π-aryl complex that allows the catalyst to stay associated to the growing polymer chain and "walks" toward the next carbon halide bond to initiate intramolecular oxidative addition. While recent improvements to CTP have focused on its mechanism, one aspect that has not been investigated is the utilization of multimetallic cooperative catalysts. Using more than one metal center that can form a stable associative interaction with the growing polymer chain can potentially overcome issues with catalyst dissociation seen with electron deficient systems.

Our previous studies to explore the use of bimetallic nickel complexes gave us insight on what structural features to employ for catalyst design. While we designed catalysts based on a

benzene diamine ligand that emulated Ni(dppp)Cl_2, a commonly employed catalyst for CTP, the increased sterics due to their different geometry resulted in reduced controlled polymerizations.[72] Additionally, two polymer chains were growing instead of one. To modify the design, we thought of changing the orientation of the coordination spheres of the metal to potentially mitigate the formation of two polymers (**Figure 5.1**). Another change that was made in the structure was replacing the nitrogen atom with carbon. This structural change was made to see if electronics played a role in the reduced performance in the previous benzene amine catalyst. As a consequence of replacing the nitrogen atom, the difficulty to synthesize the bimetallic catalyst increased.

The explored catalyst was inspired from bimetallic catalysts with rigid geometries that oriented both metal sites in the same direction either through a cofacial arrangement or double-decker structure (**Figure 5.2**).[39,73] These catalysts exhibited high catalytic activity in olefin polymerizations resulting in polymers with high molecular weight and control in branching. For our study, the orientation of two metal centers is geometric designed worth considering for CTP to potentially provide an additional stabilization effect of the metal π-aryl complex (**Figure 5.3**). The design of orienting the coordination spheres in the same direction greatly matches what we originally envisioned for creating an additional metal-polymer interaction.

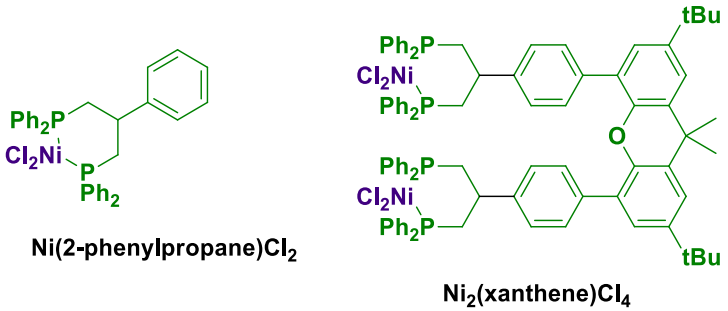

Figure 5.1. Explored catalysts in this study.

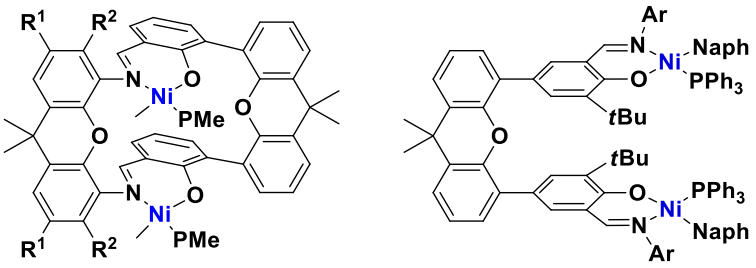

Figure 5.2. Structures of bimetallic catalysts used for olefin polymerizations.[39,73]

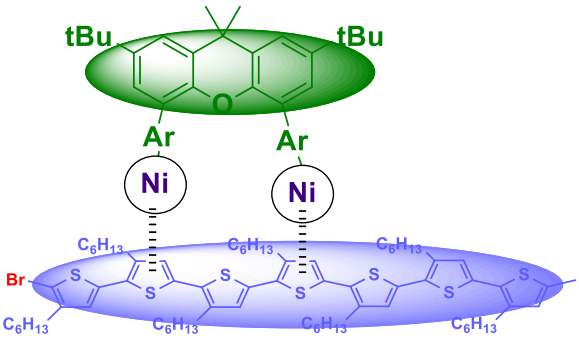

Figure 5.3. Hypothesized bimetallic π-aryl complex.

5.2 EXPERIMENTAL

5.2.1 *Synthesis of phosphine ligands*

Synthesis of the phosphine ligands are outlined in **Figure 5.4** and **5.5**.[74–79] All reagents were obtained from commercial suppliers (Sigma-Aldrich, Fisher Scientific, ACROS, VWR, TCI) and unless noted, were used as received without further purification. Solvents were obtained from Pure Solv dry stills or redistilled before use. Reactions were carried out using Schlenk lines or in a glovebox under N_2 when necessary. All synthesized compounds were purified through standard techniques, such as column chromatography, recrystallization, extraction, or filtration, and characterized using ^{1}H-NMR to confirm identity.

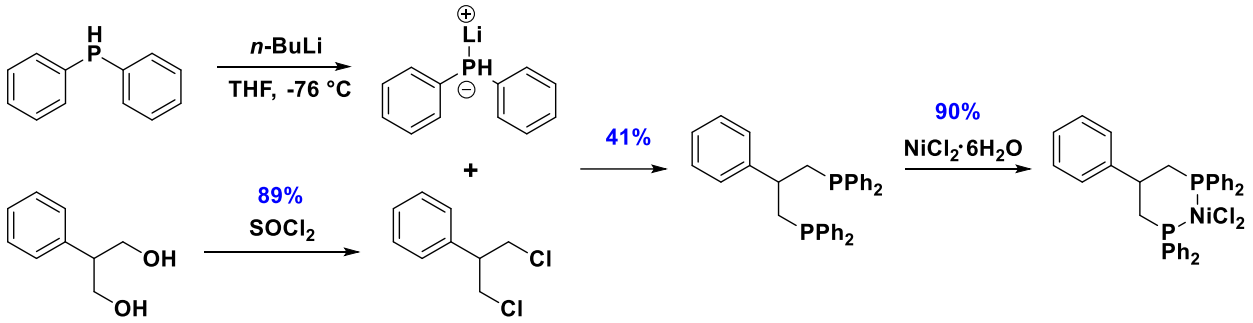

Figure 5.4. Synthesis of Ni(2-phenylpropane)Cl_2.

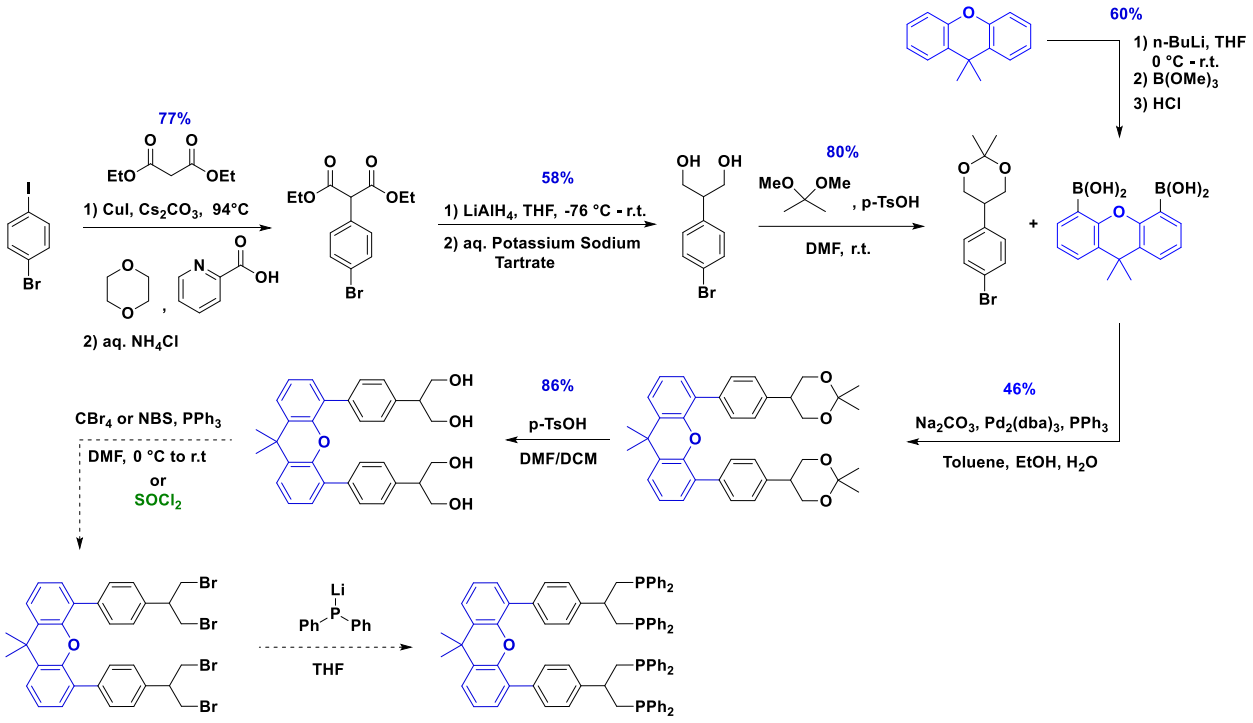

Figure 5.5. Synthesis of xanthene tetraphosphino ligand.

5.2.2 *Synthesis of P3HT via KCTP and polymer kinetics*

The polymerization kinetics follows the same established procedures in Chapter 4 (Sections 4.2.5 – 4.2.6) (**Figure 5.6**). Monomer conversion and molecular weight were determined using ^{1}H-NMR. End-group identity, chain-growth behavior, and dispersity were analyzed by MALDI-TOF MS and SEC.

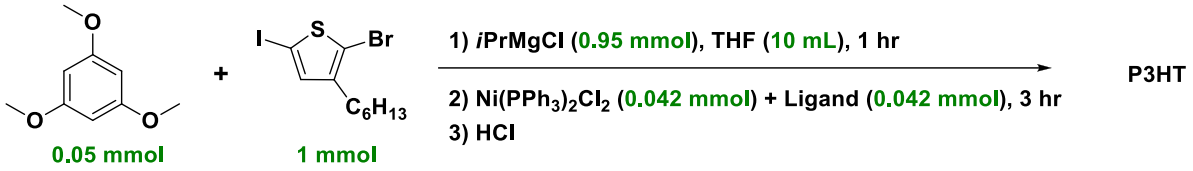

Figure 5.6. General scheme for P3HT synthesis

5.3 Results and Discussion

5.3.1 *Analysis of KCTP initiated with Ni(2-phenylpropane)Cl₂*

Figure 5.7 and **Table 5.1** summarize the polymerization kinetics with Ni(2-phenylpropane)Cl_2. For the percent monomer remaining *vs* time plot, the triplicate kinetic polymerizations of Ni(2-phenylpropane)Cl_2 were compared with the previously obtained data from Ni(dppp)Cl_2 and Ni(Aniline)Cl_2. Monomer conversions from KCTP initiated with Ni(2-phenylpropane)Cl_2 are very similar with the other two catalysts. The observed $Đ$ for Ni(2-phenylpropane)Cl_2 are higher compared to Ni(dppp)Cl_2, indicating a reduced controlled polymerization.

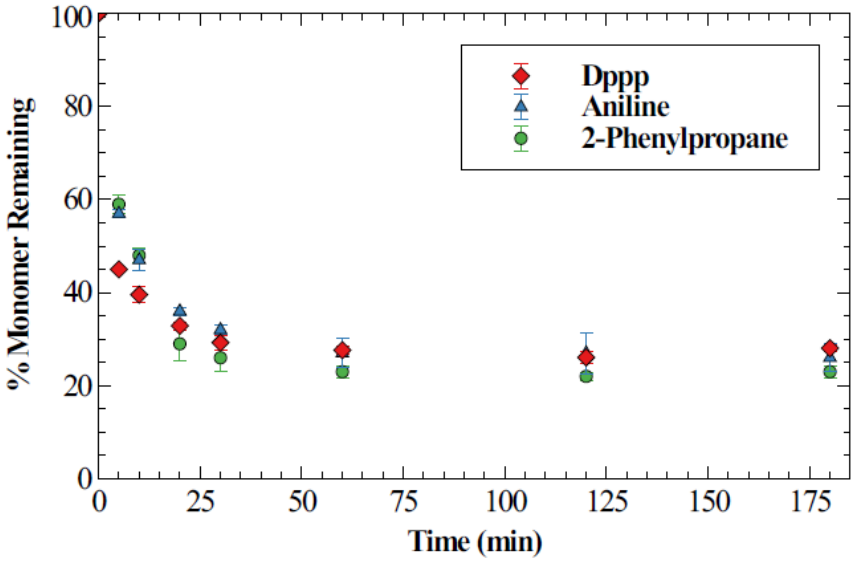

Figure 5.7. Percent monomer remaining *vs.* time plot of (3-HT) kinetic trials with error bars showing standard deviation.

Table 5.1. Results of (3-HT) polymerization trials with Ni(2-phenylpropane).

Entry	Ligand	Monomer Conversion (%)	Predicted M_n (kg/mol)	Actual M_n (kg/mol)	DP	$Đ$	Yield (%)
1	2-phenylpropane	78	3.3	3.0	20	1.60	64
2	2-phenylpropane	76	3.1	3.0	18	1.59	73
3	2-phenylpropane	80	3.9	3.0	20	1.90	83
4[a)]	dppp	74	3.1	3.0	19	1.25	68
5[a)]	aniline	75	2.9	3.0	18	1.85	67

[a)] Reported values represent the averages of the previous triplicate studies

MALDI-TOF MS was used to ascertain the distribution of end-groups of the isolated P3HT (**Figure 5.8**). Ni(2-phenylpropane) (Figure 5.5b) shows increased chain termination through the higher content of Br/Br P3HT. This result makes it comparable to Ni(Aniline)Cl_2 (Figure 5.8a) and provides additional evidence on a reduced controlled polymerization. The results shown in the are very similar to what has been previously observed with these catalyst studies. It appears that replacing the nitrogen atom with carbon did not make a significant difference in the polymerizations, suggesting that sterics is playing a major role and not electronics. However, it is worth noting that phenyl groups are inductively electron withdrawing, which may influence the metal π-aryl complex due to less electron density on the metal.[20] This reasoning was previously used in potentially explaining the reactivity of Ni(Aniline)Cl_2 with the nitrogen atom donating its electron density in resonance to the benzene ring. Catalysts that lack have decreased electron density perform worse in CTP as the strength of the π interaction between the metal and polymer is weakened.

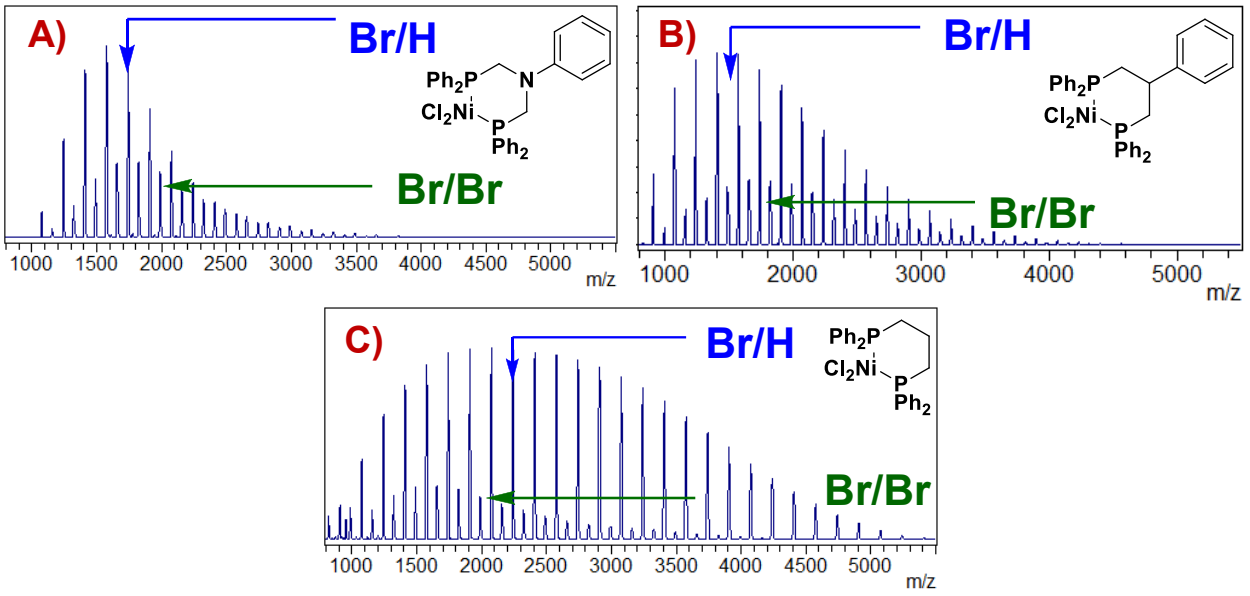

Figure 5.8. MALDI-TOF data for (3-HT) KCTP polymerization. (A) Ni(Aniline)Cl_2; (B) Ni(2-phenylpropane)Cl_2; (C) Ni(dppp)Cl_2.

5.3.2 *Analysis of the structure of Ni(2-phenylpropane)Cl_2*

Ni(2-phenylpropane)Cl_2 was synthesized using $NiCl_2$ hexahydrate and X-ray quality crystals was generated using vapor diffusion recrystallization in methylene chloride and cyclopentane. The crystal structure of Ni(2-phenylpropane)Cl_2 is displayed in **Figure 5.9**. From this crystal structure, the reported bite angle of Ni(2-phenylpropane)Cl_2 is 96.5°. **Table 5.2** compares the bite angles of the Ni(Aniline)Cl_2, Ni(2-phenylpropane)Cl_2 and Ni(dppp)Cl_2. With the larger bite angle, we can infer that Ni(2-phenylpropane)Cl_2 would have a larger cone angle. One would expect that Ni(2-phenylpropane)Cl_2 would perform worse in CTP, due to increased sterics from the ligand, however that is not the case as it performs on par with Ni(Aniline)Cl_2 and creates P3HT with slightly lower dispersity. This finding indicates that chain-termination is occurring at a step that does not involve the metal π-aryl complex.

The two chain-termination processes that can occur in KCTP that can form Br/Br end-groups on P3HT are catalyst dissociation and disproportionation. Catalyst dissociation can result from an unstable metal π-aryl complex while disproportionation can occur during TM as a competing process against the organomagnesio compound. Analysis of the GPC profiles where tailing or presence of a shoulder peak at a higher molecular weight indicate disproportionation. Additionally, the presence of a H-H coupling can be identified in ^{1}H-NMR by viewing the signal at the methylene proton region at 2.5 ppm.

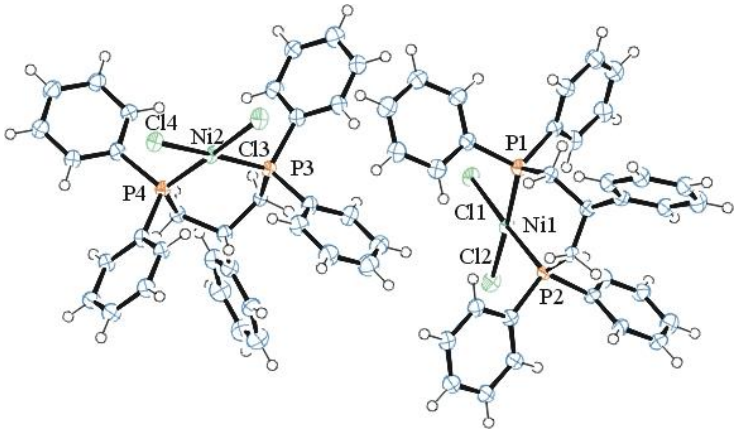

Figure 5.9. ORTEP of Ni(2-phenylpropane)Cl_2 with thermal ellipsoids at the 50% probability.

Table 5.2. Comparison of ligand P-M-P bite angles.

Ligand	dppp	Aniline	2-phenylpropane
Bite Angle	91.77°	94.89°	96.5°
Cone Angle	142°	>142°	>142°

5.4 CONCLUSION

From the work that has been completed so far, Ni(2-phenylpropane)Cl_2 exhibited similar catalytic activity to Ni(aniline)Cl_2 from the previous study. Both catalysts exhibit more chain termination processes compared to Ni(dppp)Cl_2. Despite having a larger bite angle and cone angle, Ni(2-phenylpropane)Cl_2 does not perform significantly worse compared Ni(2-phenylpropane)Cl_2,

indicating that the steric bulk of the ligand appears to have no effect on catalyst performance. The stability of the metal π-aryl complex has no effect on disproportionation since this competing side process occurs after intramolecular oxidative addition. Disproportionation is fundamentally a transmetalation, so it is interesting that Ni(2-phenylpropane)Cl_2 and Ni(aniline)Cl_2 are performing similarly despite the difference in steric bulk of the phosphine ligands. The results of this study points towards disproportionation as the contributing factor to increased Br/Br terminated P3HT.

5.5 FUTURE WORK

One potential avenue to explore that will solve whether electronics is playing a role in catalyst behavior involve a complex that contains an electron-donating group. Previous investigations in CTP that changed the electronics on the catalyst focused on the attenuating the aryl phosphine. The studies in this work have the electronic group on the bidentate part of the ligand. Putting an alkoxy group on the *para* position of the phenyl ring would be a simple and suitable candidate to answer the conundrum with electronics *vs* sterics.

Since disproportionation is likely occurring over catalyst dissociation, a next step in this study would involve determining the disproportionation energy (E_{disp}) of the catalysts used in KCTP. E_{disp} is a thermodynamic quantity calculated using DFT that influences the likelihood of disproportionation occurring in the polymerization.[66] Bilbrey *et al.* conducted a study that included bidentate phosphine ligands and concluded that E_{disp} had a major impact on the success of the polymerization over catalyst geometry. This may be the case for Ni(aniline)Cl_2 and Ni(2-phenylphosphine)Cl_2, since the changes in sterics did not lead to any difference in catalyst behavior. This may not be the same for the bimetallic catalysts, since steric clash of the growing polymer chain was present and prevented the polymer from growing beyond a certain chain length.

The synthesis of the xanthene ligand is currently underway. We hope to finish the synthesis and run the final polymerization tests to determine whether the orientation of the two metal centers will benefit CTP.

Chapter 6. FUTURE OUTLOOK FOR MULTIMETALLIC CATALYSIS IN CTP

Catalyst-transfer polymerization has greatly expanded the field of π-conjugated polymers, affording a vast network of polymeric architectures. Further advances in the area have been impeded by the limited monomer scope, with simple and electron-rich monomers as the common substrates. There has also been a disparity between the structural diversification of monomers and suitable catalysts that retain controlled polymerizations. Despite all the mechanistic insight obtained in CTP, the improvement in catalyst efficiency has remained stunted. The catalyst-monomer interaction is an essential component in CTP that can vary depending on the ligands and transmetalating agents. Designing a suitable catalyst that will exhibit controlled polymerizations is challenging due to the diversity in catalyst-monomer interactions. This is especially so for electron-deficient monomers.

Multimetallic catalysis has potential to improve CTP in that it focuses on the catalyst-monomer interaction. However, it has its challenges. 1) Designing a bimetallic precatalyst with a preorganized structure is no simple feat. The examples in the literature that have been used for olefin and epoxide polymerizations are complex and require long syntheses. Due to their overall complexity, screening suitable bimetallic catalysts for CTP is a much more arduous process compared to monometallic systems. 2) Getting the metal sites to work cooperatively together is difficult as shown in this study where two polymer chains were growing on the bimetallic Ni complexes. Additionally, the oxidation of the metal is something to consider. The precatalysts used in this study are in their M(II) oxidation states. To obtain the desired cooperative effects, both metal centers need to be in their M(0) species form. A potential solution to circumvent this issue is to use a M(0) precatalyst, however known examples, such as $Pd(PPh_3)_4$ and $Ni(COD)_2$, are

known for their instability. A recent paper by Nattmann and coworkers in Nature Catalysis has resulted in the creation of an air stable binary Ni(0) precatalyst.[80] This system may be useful for CTP. If these challenges can be overcome, then the potentiality of multimetallic catalysis in CTP can be fully explored.

REFERENCES

(1) Yokoyama, A.; Miyakoshi, R.; Yokozawa, T. *Macromolecules* **2004**, *37* (4), 1169–1171.

(2) Sheina, E. E.; Liu, J.; Lovu, M. C.; Laird, D. W.; McCullough, R. D. *Macromolecules* **2004**, *37* (10), 3526–3528.

(3) Huang, Y.; Zheng, N.; Wang, Z.; Ying, L.; Huang, F.; Cao, Y. *Chem. Commun.* **2017**, *53* (12), 1997–2000.

(4) Mazzio, K. A.; Rice, A. H.; Durban, M. M.; Luscombe, C. K. *J. Phys. Chem. C* **2015**, *119* (27), 14911–14918.

(5) Vangerven, T.; Verstappen, P.; Drijkoningen, J.; Dierckx, W.; Himmelberger, S.; Salleo, A.; Vanderzande, D.; Maes, W.; Manca, J. V. *Chem. Mater.* **2015**, *27* (10), 3726–3732.

(6) Monnaie, F.; Verheyen, L.; De Winter, J.; Gerbaux, P.; Brullot, W.; Verbiest, T.; Koeckelberghs, G. *Macromolecules* **2015**, *48* (24), 8752–8759.

(7) Yokozawa, T.; Ohta, Y. *Chem. Rev.* **2016**, *116* (4), 1950–1958.

(8) Bryan, Z. J.; McNeil, A. J. *Macromolecules* **2013**, *46* (21), 8395–8405.

(9) Leone, A. K.; McNeil, A. J. *Acc. Chem. Res.* **2016**, *49* (12), 2822–2831.

(10) Tkachov, R.; Senkovskyy, V.; Komber, H.; Sommer, J. U.; Kiriy, A. *J. Am. Chem. Soc.* **2010**, *132* (22), 7803–7810.

(11) Verheyen, L.; Leysen, P.; Van Den Eede, M. P.; Ceunen, W.; Hardeman, T.; Koeckelberghs, G. *Polym. (United Kingdom)* **2017**, *108*, 521–546.

(12) Nanashima, Y.; Yokoyama, A.; Yokozawa, T. *Macromolecules* **2012**, *45* (5), 2609–2613.

(13) Nanashima, Y.; Yokoyama, A.; Yokozawa, T. *J. Polym. Sci. Part A Polym. Chem.* **2012**, *50* (6), 1054–1061.

(14) Govaerts, S.; Verstappen, P.; Penxten, H.; Defour, M.; Van Mele, B.; Lutsen, L.;

Vanderzande, D.; Maes, W. *Macromolecules* **2016**, *49* (17), 6411–6419.

(15) Bridges, C. R.; McCormick, T. M.; Gibson, G. L.; Hollinger, J.; Seferos, D. S. *J. Am. Chem. Soc.* **2013**, *135* (35), 13212–13219.

(16) Hou, J.; Chen, H. Y.; Zhang, S.; Chen, R. I.; Yang, Y.; Wu, Y.; Li, G. *J. Am. Chem. Soc.* **2009**, *131* (43), 15586–15587.

(17) Müllen, K.; Pisula, W. *J. Am. Chem. Soc.* **2015**, *137* (30), 9503–9505.

(18) Holliday, S.; Li, Y.; Luscombe, C. K. *Prog. Polym. Sci.* **2017**, *70*, 34–51.

(19) Lanni, E. L.; McNeil, A. J. *Macromolecules* **2010**, *43* (19), 8039–8044.

(20) Lee, S. R.; Bryan, Z. J.; Wagner, A. M.; McNeil, A. J. *Chem. Sci.* **2012**, *3* (5), 1562-1566.

(21) Lanni, E. L.; Locke, J. R.; Gleave, C. M.; McNeil, A. J. *Macromolecules* **2011**, *44* (13), 5136–5145.

(22) Mikami, K.; Nojima, M.; Masumoto, Y.; Mizukoshi, Y.; Takita, R.; Yokozawa, T.; Uchiyama, M. *Polym. Chem.* **2017**, *8* (10), 1708–1713.

(23) Leone, A. K.; Souther, K. D.; Vitek, A. K.; LaPointe, A. M.; Coates, G. W.; Zimmerman, P. M.; McNeil, A. J. *Macromolecules* **2017**, *50* (23), 9121–9127.

(24) Tetyana Beryozkina, Volodymyr Senkovskyy, Elisabeth Kaul, and A. K. *J. Mater. Chem. A* **2008**, *41* (21), 7817–7823.

(25) Baker, M. A.; Ayuso-Carrillo, J.; Koos, M. R. M.; MacMillan, S. N.; Varni, A. J.; Gil, R. R.; Noonan, K. J. T. *Polym. J.* **2019**.

(26) Ye, S.; Foster, S. M.; Pollit, A. A.; Cheng, S.; Seferos, D. S. *Chem. Sci.* **2019**, *10* (7), 2075–2080.

(27) Lanni, E. L.; Mcneil, A. J. *J. Am. Chem. Soc.* **2009**, *131* (13), 16573–16579.

(28) Lamps, J. P.; Catala, J. M. *Macromolecules* **2011**, *44* (20), 7962–7968.

(29) Wu, S.; Huang, L.; Tian, H.; Geng, Y.; Wang, F. *Macromolecules* **2011**, *44* (19), 7558–7567.

(30) Yokozawa, T.; Nanashima, Y.; Ohta, Y. *ACS Macro Lett.* **2012**, *1* (7), 862–866.

(31) Komber, H.; Senkovskyy, V.; Tkachov, R.; Johnson, K.; Kiriy, A.; Huck, W. T. S.; Sommer, M. *Macromolecules* **2011**, *44* (23), 9164–9172.

(32) Karpov, Y.; Maiti, J.; Tkachov, R.; Beryozkina, T.; Bakulev, V.; Liu, W.; Komber, H.; Lappan, U.; Al-Hussein, M.; Stamm, M.; et al. *Polym. Chem.* **2016**, *7* (15), 2691–2697.

(33) Smith, M. L.; Leone, A. K.; Zimmerman, P. M.; McNeil, A. J. *ACS Macro Lett.* **2016**, *5* (12), 1411–1415.

(34) Willot, P.; Koeckelberghs, G. *Macromolecules* **2014**, *47* (24), 8548–8555.

(35) Bilbrey, J. A.; Bootsma, A. N.; Bartlett, M. A.; Locklin, J.; Wheeler, S. E.; Allen, W. D. *J. Chem. Theory Comput.* **2017**, *13* (4), 1706–1711.

(36) Nojima, M.; Ohta, Y.; Yokozawa, T. *J. Polym. Sci. Part A Polym. Chem.* **2014**, *52* (18), 2643–2653.

(37) Liu, S.; Motta, A.; Mouat, A. R.; Delferro, M.; Marks, T. J. *J. Am. Chem. Soc.* **2014**, *136* (29), 10460–10469.

(38) Zhu, L.; Fu, Z. S.; Pan, H. J.; Feng, W.; Chen, C.; Fan, Z. Q. *Dalt. Trans.* **2014**, *43* (7), 2900–2906.

(39) Chen, Z.; Yao, E.; Wang, J.; Gong, X.; Ma, Y. *Macromolecules* **2016**, *49* (23), 8848–8854.

(40) Lobkovsky, E. B.; Ahmed, S. M.; Hirahata, W.; Widger, P. C. B.; Thomas, R. M.; Coates, G. W.; Jeske, R. C.. *J. Am. Chem. Soc.* **2010**, *132* (46), 16520–16525.

(41) Peris, E. *Chem. Rev.* **2018**, *118* (19), 9988–10031.

(42) Kirmse, W. *Angew. Chemie - Int. Ed.* **2004**, *43* (14), 1767–1769.

(43) Antonova, N. S.; Carbó, J. J.; Poblet, J. M. *Organometallics* **2009**, *28* (15), 4283–4287.

(44) Xi, Z.; Zhang, X.; Chen, W.; Fu, S.; Wang, D. *Organometallics* **2007**, *26* (26), 6636–6642.

(45) Zhou, Y.; Xi, Z.; Chen, W.; Wang, D. *Organometallics* **2008**, *27* (22), 5911–5920.

(46) Xi, Z.; Liu, B.; Chen, W. *J. Org. Chem.* **2008**, *73* (10), 3954–3957.

(47) Hopkinson, M. N.; Richter, C.; Schedler, M.; Glorius, F. *Nature* **2014**, *510* (7506), 485–496.

(48) Raba, A.; Anneser, M. R.; Jantke, D.; Cokoja, M.; Herrmann, W. A.; Kühn, F. E. *Tetrahedron Lett.* **2013**, *54* (26), 3384–3387.

(49) Schenck, T. G.; Downes, J. M.; Milne, C. R. C.; Mackenzie, P. B.; Boucher, H.; Whelan, J.; Bosnich, B. *Inorg. Chem.* **1985**, *24* (15), 2334–2337.

(50) Deckers, S.; Vandendriessche, S.; Cornelis, D.; Monnaie, F.; Koeckelberghs, G.; Asselberghs, I.; Verbiest, T.; Van Der Veen, M. A. *Chem. Commun.* **2014**, *50* (21), 2741–2743.

(51) Qiu, Y.; Worch, J. C.; Fortney, A.; Gayathri, C.; Gil, R. R.; Noonan, K. J. T. *Macromolecules* **2016**, *49* (13), 4757–4762.

(52) Qiu, Y.; Mohin, J.; Tsai, C. H.; Tristram-Nagle, S.; Gil, R. R.; Kowalewski, T.; Noonan, K. J. T. *Macromol. Rapid Commun.* **2015**, *36* (9), 840–844.

(53) Bryan, Z. J.; Hall, A. O.; Zhao, C. T.; Chen, J.; McNeil, A. J. *ACS Macro Lett.* **2016**, *5* (1), 69–72.

(54) Ruiz-Botella, S.; Peris, E. *Organometallics* **2014**, *33* (19), 5509–5516.

(55) Leone, A. K.; Mueller, E. A.; McNeil, A. J. *J. Am. Chem. Soc.* **2018**, *140* (45), 15126–

15139.

(56) Sook, K. K.; Moon, B. S.; Ju, H. P.; Young, I. S.; Hwa, S. K.; Yeo, J. Y.; Lee, K. D.; Yoon, J. *Tetrahedron Lett.* **2005**, *46* (39), 6617–6620.

(57) Wang, K.; Wang, W.; Luo, H.; Zheng, X.; Fu, H.; Chen, H.; Li, R. *Catal. Letters* **2013**, *143* (11), 1214–1219.

(58) Uruş, S.; İncesu, M.; Köşker, S.; Kurt, A. H.; Ceyhan, G. *Appl. Organomet. Chem.* **2017**, *31*, e3550.

(59) Fawcett, J.; Hoye, P. A. T.; Kemmitt, R. D. W.; Law, D. J.; Russel, D. R. *J. Chem. Soc. Dalt. Trans.* **1993**, No. 1, 2563–2568.

(60) Dohi, T.; Yamaoka, N.; Nakamura, S.; Sumida, K.; Morimoto, K.; Kita, Y. *Chem. - A Eur. J.* **2013**, *19* (6), 2067–2075.

(61) Hu, Y.; Ivaturi, A.; Planells, M.; Boldrini, C. L.; Biroli, A. O.; Robertson, N. *J. Mater. Chem. A* **2016**, *4* (7), 2509–2516.

(62) Beryozkina, T.; Senkovskyy, V.; Kaul, E.; Kiriy, A. *Macromolecules* **2008**, *41* (21), 7817–7823.

(63) Standley, E. A.; Smith, S. J.; Müller, P.; Jamison, T. F. *Organometallics* **2014**, *33* (8), 2012–2018.

(64) Iovu, M. C.; Sheina, E. E.; Gil, R. R.; Mccullough, R. D. *Macromolecules*. **2005**, 8649–8656.

(65) Pouliot, J.; Wakioka, M.; Ozawa, F.; Li, Y.; Leclerc, M. *Macromol. Chem. Phys.* **2016**, *217* (13), 1493–1500.

(66) Bilbrey, J. A.; Sontag, S. K.; Huddleston, N. E.; Allen, W. D.; Locklin, J. *ACS Macro Lett.* **2012**, *1* (8), 995–1000.

(67) Tkachov, R.; Senkovskyy, V.; Komber, H.; Kiriy, A. *Macromolecules* **2011**, *44* (7), 2006–2015.

(68) Nojima, M.; Ohta, Y.; Yokozawa, T. *J. Am. Chem. Soc.* **2015**, *137* (17), 5682–5685.

(69) Seyler, H.; Subbiah, J.; Jones, D. J.; Holmes, A. B.; Wong, W. W. H. **2013**, *J. Org. Chem.* **2013**, *9*, 1492–1500.

(70) Blake, A. V.; Donahue, C. M.; McCollom, S. P.; Keith, J. M.; Forrest, C. M.; Daly, S. R.; Bellott, B. J. *Inorg. Chem.* **2015**, *54* (12), 5646–5659.

(71) Niksch, T.; Görls, H.; Weigand, W. *Eur. J. Inorg. Chem.* **2010**, *2010*, 95–105.

(72) Hardeman, T.; Willot, P.; Winter, J. De; Josse, T.; Gerbaux, P.; Shestakova, P.; Nies, E.; Koeckelberghs, G. *J. Polym. Sci. Part A Polym. Chem.* **2014**, *52* (6), 804–809.

(73) Takeuchi, D.; Chiba, Y.; Takano, S.; Kurihara, H.; Kobayashi, M.; Osakada, K. *Polym. Chem.* **2017**, *8* (34), 5112–5119.

(74) Doherty, S.; Robins, E. G.; Nieuwenhuyzen, M.; Champkin, P. A.; Clegg, W. *Organometallics* **2002**, *21* (20), 4147–4158.

(75) Carter, A.; Mason, A.; Baker, M. A.; Bettler, D. G.; Changas, A.; McMillen, C. D.; Tapu, D. *Organometallics* **2017**, *36* (9), 1867–1872.

(76) Katz, C. E.; Aubé, J. *J. Am. Chem. Soc.* **2003**, *125* (46), 13948–13949.

(77) Rew, Y.; Du, X.; Eksterowicz, J.; Zhou, H.; Jahchan, N.; Zhu, L.; Yan, X.; Kawai, H.; McGee, L. R.; Medina, J. C.; et al. *J. Med. Chem.* **2018**, *61* (17), 7767–7784.

(78) Wang, R.; Sui, X.; Pang, W.; Chen, C. *ChemCatChem* **2016**, *8* (2), 434–440.

(79) Hirotsu, M.; Ohno, N.; Nakajima, T.; Kushibe, C.; Ueno, K.; Kinoshita, I. *Dalt. Trans.* **2010**, *39* (1), 139–148.

(80) Nattmann, L.; Saeb, R.; Cornella, J. *Nat. Catal.* **2019**.

APPENDIX A

Equations used in polymerization studies

$$DP = \left(\frac{I_{repeating\ unit}}{\#\ of\ protons\ of\ repeating\ unit} \times \frac{\#\ of\ protons\ of\ end-groups}{I_{end-groups\ and\ regioisomers}}\right) + 2 \quad (1)$$

$$n = \left(\frac{[M_i]}{[Ni_i]}\right) \quad (2)$$

$$M_{n(Predicted)} = n \times (M.W.of\ repeating\ unit) \quad (3)$$

VITA

PROFESSIONAL EXPERIENCE

2014 – Present	**PhD Candidate in Chemistry**
	University of Washington – Luscombe Lab:
2017 – 2018	**Instructor in Organic Chemistry**
	University of Washington, Summer Health Professions Education Program
2013 – 2014	**Research Associate/Lab Manager**
	California State University, Los Angeles – Tunstad Lab
2011 – 2013	**MS Graduate Student Research Assistant**
	California State University, Los Angeles – Tunstad Lab
2008 – 2010	**Student Research Assistant**
	University of California, Los Angeles – Garcia-Garibay Lab
2009	**Student Research Assistant**
	University of California, Berkeley – Sarpong Lab

AWARDS & FELLOWSHIPS

2019	University of Washington Alumni Association Homecoming Scholar
2019	Excellence in Teaching Award Recipient
2019	Husky 100
2018	Excellence in Teaching Award Finalist
2016	Phi Lambda Upsilon: UW Chemistry Honor Society Teaching Award
2012, 2013	California State University, Los Angeles Annual Honors Convocation – Special Recognition in Graduate Studies
2011	Minority Biomedical Research Support-Research Initiative for Scientific Enhancement Graduate Fellowship
2008	University of California's Leadership Excellence through Advanced Degrees Fellowship

LEADERSHIP & CIVIC ACTIVITIES

2014 - 2019	Lead Officer: President & Historian/Webmaster *UW Society for the Advancement of Chicanos/Hispanics and Native Americans in Science*
2016 – 2017	RSO/Outreach Lead *Diversity in Clean Energy*

COMMUNICATION

Presentation

2019	American Chemical Society Fall National Meeting, San Diego, CA.

Publications

2019	"Investigation of Bimetallic Nickel Catalysts in Catalyst-Transfer Polymerization of π-Conjugated Polymers" *Macromol. Chem. Phys.* **2019**, 1900363.
2019	"Living polymerizations of π-conjugated semiconductors", Handbook of Conducting Polymers, Fourth Edition, Two-Volume Set, CRC Press/Taylor & Francis, **2019**, DOI:[10.1201/b22235-6].
2016	"Crystal Fluidity Reflected by Fast Rotational Motion at the Core, Branches, and Peripheral Aromatic Groups of a Dendrimeric Molecular Rotor. *J. Am. Chem. Soc.* **2016**, *138*, 4650–4656.
2013	"Biscavitand model systems for surface recognition and self-assembling Oligomers" M.S. Thesis, California State University, Los Angeles.

Jeffrey Paz Buenaflor was born and raised in San Diego, CA. He graduated from Southwest Senior High School in 2006 ranked #4 in his class. Afterwards, he moved to Los Angeles to attend UCLA, graduating in 2010 with a BS in biochemistry. Jeffrey would later return to Los Angeles to obtain his MS in chemistry at CSULA in 2013. In the fall of 2014, Jeffrey relocated to Seattle to pursue his dream of obtaining a PhD at the University of Washington.